



**HAL**  
open science

## New insights in Neanderthal palaeoecology using stable oxygen isotopes preserved in small mammals as palaeoclimatic tracers in Teixoneres Cave (Moià, northeastern Iberia).

Monica Fernández-García, J.M. López-García, Aurélien Royer, Christophe Lécuyer, F. Rivals, A. Rufà, R. Blasco, J. Rosell

### ► To cite this version:

Monica Fernández-García, J.M. López-García, Aurélien Royer, Christophe Lécuyer, F. Rivals, et al.. New insights in Neanderthal palaeoecology using stable oxygen isotopes preserved in small mammals as palaeoclimatic tracers in Teixoneres Cave (Moià, northeastern Iberia).. *Archaeological and Anthropological Sciences*, 2022, 14 (6), pp.106. 10.1007/s12520-022-01564-9 . hal-03678918

**HAL Id: hal-03678918**

**<https://hal.science/hal-03678918>**

Submitted on 30 May 2022

**HAL** is a multi-disciplinary open access archive for the deposit and dissemination of scientific research documents, whether they are published or not. The documents may come from teaching and research institutions in France or abroad, or from public or private research centers.

L'archive ouverte pluridisciplinaire **HAL**, est destinée au dépôt et à la diffusion de documents scientifiques de niveau recherche, publiés ou non, émanant des établissements d'enseignement et de recherche français ou étrangers, des laboratoires publics ou privés.



Distributed under a Creative Commons Attribution 4.0 International License



# New insights in Neanderthal palaeoecology using stable oxygen isotopes preserved in small mammals as palaeoclimatic tracers in Teixoneres Cave (Moià, northeastern Iberia)

M. Fernández-García<sup>1</sup> · J. M. López-García<sup>2,3</sup> · A. Royer<sup>4</sup> · C. Lécuyer<sup>5,6</sup> · F. Rivals<sup>2,3,7</sup> · A. Rufà<sup>8,9</sup> · R. Blasco<sup>2,3</sup> · J. Rosell<sup>3,2</sup>

Received: 4 December 2021 / Accepted: 25 April 2022  
© The Author(s) 2022

## Abstract

The northeastern region of Iberia constitutes a natural pass-area for arriving populations into the peninsula and becomes a key area to understand Neanderthal resilience to changing environmental conditions experienced during Marine Isotope Stage 3 (MIS 3; 60–30 ka). Short-term but repeated occupations by Neanderthal groups occurred in Teixoneres Cave (Moià, Barcelona) in alternation with large and small carnivores during MIS3. Abundant small-mammal remains accumulated in units III and II of this fossiliferous deposit, providing local climatic and environmental information. This work focuses on the taphonomic history of small-mammal faunas, which is a clue to validate previous palaeoecological interpretations. As was observed with leporids and bird remains, raptors are considered the major source of small-mammal remains. The most likely accumulator is an opportunistic predator, the eagle owl, with very rare inputs by mammalian carnivores. In parallel, high-resolution palaeoclimatic data are provided through oxygen isotope analyses ( $\delta^{18}\text{O}$ ) of rodent teeth from four subunits (IIIb to IIa), which are compared with independent methods of palaeotemperature estimations. According to air temperatures estimated from  $\delta^{18}\text{O}$  rodent teeth, cooler conditions than present day ( $-1.6/-0.5\text{ }^{\circ}\text{C}$ ) are recorded along the sequence, but homogenous ( $<1\text{ }^{\circ}\text{C}$ ). Complementary methods also explain higher rainfall than present day ( $+44/+682\text{ mm}$ ). Only slight changes between units III and II show climatic instability, which could be related to palimpsests of stadial-interstadial events. Climatic stable conditions are reported from coeval isotopic and palaeodiet analyses from northeastern Iberia in agreement with the palynological records that underline how the Mediterranean area could have sustained rich ecosystems that assured the Neanderthal subsistence during the abrupt climatic pulsations of the Late Glacial.

**Keywords** Middle Palaeolithic · Southwestern Europe · Palaeoenvironment · Geochemistry · Taphonomy

## Introduction

Southern European peninsulas are key areas to understand Neanderthal resilience to changing environmental conditions experienced during Marine Isotopic Stage 3 (MIS 3; ca. 60–30 ka). This period is characterized by intense climatic fluctuations, reflected in global ice and marine proxies (Fletcher and Sánchez-Goñi 2008; Fletcher et al. 2010a; Wolff et al. 2010; Moreno et al. 2014; Rasmussen et al. 2014), and coincides with the most extensive Neanderthal occupations reflected by the archaeological record in Iberia,

along with their substitution by anatomical modern humans at the end of this period (Maroto et al. 2012; Higham et al. 2014; Wood et al. 2014; Marín-Arroyo et al. 2018). Climate, even if not the unique cause, should have an influence on the exploitation and occupation of their territory, conditioning hunting areas and the availability of vegetable resources (Zilhão 2000, 2006; D’Errico and Sánchez Goñi 2003; Finlayson et al. 2006; Finlayson and Carrión 2007). The Iberian Peninsula is a particularly interesting region considering its buffered climatic conditions compared to northern latitudes, but at the same time sheltering highly diverse microenvironments derived from their complex orography (Hewitt 2000; Sommer and Nadachowski 2006; Stewart et al. 2010; Jones 2021). Due to its geographic position, the northeastern region of the Iberian Peninsula became a natural pass-area for arriving populations and the primary connection

✉ M. Fernández-García  
monica.fernandez.garcia.90@gmail.com

Extended author information available on the last page of the article

with the rest of Eurasia through the Mediterranean corridor. Evaluating the degree of adaptation of the Neanderthal groups in this region is essential to understand how they could face future human population arrivals. To provide reliable local-to-regional palaeoclimatic reconstructions of Middle Palaeolithic sites, especially in quantifiable terms that allow regional-to-global comparisons, it is essential to reach a deep knowledge in the ecological conditions faced by the Neanderthals during the millennia before the arrival of anatomically modern humans.

Teixoneres Cave preserves a well-studied fossiliferous deposit that can help to approach specific climatic conditions when Neanderthal populations were still spreading across Iberia. Neanderthal groups recurrently occupied Teixoneres Cave (Moià, Barcelona) during MIS 3, as it is attested by the Mousterian lithics recovered in the site. Carnivores such as hyenas, bears, and other small mammals, and birds of prey both nocturnal and diurnal, also frequented the cave and played an active role in the development of this sequence. These occupational dynamics were interrupted by short and sporadic Neanderthal settlements (Rosell et al. 2008, 2010a, b, 2017; Rufà et al. 2014, 2016; Sánchez-Hernández et al. 2014, 2016). Along this fossiliferous sequence, abundant small-mammal remains were accumulated, providing local climatic and environmental information. Owls, which probably roosted inside the cave over decades and centuries, are preliminarily assumed to be the main agent involved in a large number of small mammals (insectivores, bats, and rodents) in 2 sediments. However, until now, no complete taphonomic analysis was performed on this group and only some preliminary remarks were made (López-García et al. 2012a, 2014).

Accurate ecological inferences based on small mammals require complete knowledge of the agents involved in their accumulation (e.g. Andrews 1990), especially for deposits from which carnivores have frequently contributed, as is the case of Teixoneres Cave (see synthesis in Rosell et al. 2017). In this work, taphonomic analyses of small-mammal samples recovered from four subunits (IIIb, IIIa, IIb, and IIa) are presented. Apart from the identification of the main taphonomic agent involved in their accumulation, post-depositional alterations have also affected these small-mammal remains until they were recovered. A multidisciplinary team working at the site has recently provided extensive data concerning issues that can affect small-mammal assemblages, such as the origin of small prey (leporids and birds), the seasonality of the production of these remains, and the evaluation of time periods of human occupations, that should be addressed (Rufà et al. 2014, 2016; Sánchez-Hernández et al. 2014, 2016, 2020a, b; Rosell et al. 2017; Picin et al. 2020; Zilio et al. 2021).

Recent excavations in unit III have also provided interesting findings with ecological implications, such as the

occasional presence of the woolly mammoth and the woolly rhinoceros, which are two cold-adapted fauna infrequent in Iberia (Álvarez-Lao et al. 2017). Moreover, previous absolute dates (Tissoux et al. 2006) and relative chronology inferred from small-vertebrate faunas (López-García et al. 2012a) have been adjusted through new radiocarbon dates (Talamo et al. 2016). Also, with special relevance, a new and complete palynological study has been just published (Ochando et al. 2020). These new findings, in addition to expanding archaeo-palaeontological material during the ongoing excavations, allowed us to review the initial palaeoenvironmental reconstruction based on small vertebrates. This work complements previous reconstructions performed by using 40 oxygen isotope analysis ( $\delta^{18}\text{O}$ ) of rodent incisors from subunits IIIb to IIa. The relationships between  $\delta^{18}\text{O}$  preserved in mammal body tissues with  $\delta^{18}\text{O}$  of meteoric waters and mean annual temperatures allowed us to quantify the magnitude of the climatic changes through the sequence (Royer et al. 2013a, 2014; Fernández-García et al. 2019, 2020). Thus, considering all the recent research on the site, this work aims to reevaluate the ecological conditions during this sequence formation, unravelling the origins of the small-mammal remains and post-depositional processes. In addition, it presents an attempt to estimate air palaeotemperatures, based on the oxygen isotope analysis of rodent remains, and a comparison with independent methods for estimating climatic parameters. These environmental and climatic reconstructions are framed in this work within the regional-to-global ecological conditions experienced by Neanderthal populations during MIS 3 in Iberia.

## Teixoneres Cave

### Archaeological general information

Teixoneres Cave is located 5 km east of the village of Moià (Barcelona, Spain) (Fig. 1A) and belongs to the 2 km-long Toll Caves' karstic system, formed by the drainage system of the Torrent del Mal, which modelled the Neogene limestone, called Collsuspina Formation. The karst coordinates are 2°09'02"E and 41°48'25"N at 760 m a.s.l. (Rosell et al. 2008). It is located in the highlands between the two main rivers that are the Llobregat and the Ter, connecting the central region of Catalonia with the Mediterranean coast (Rosell et al. 2017). The Toll karstic complex was discovered in the 1950s by a local speleological group. Several archaeological deposits from different chronologies are contained within this complex of caves, of which Teixoneres Cave and Toll Cave are those that contain Palaeolithic assemblages (Rosell et al. 2014). Several interventions were carried out by different research teams until the 1990s in the Toll karstic complex, bringing to light an important Holocene and Late

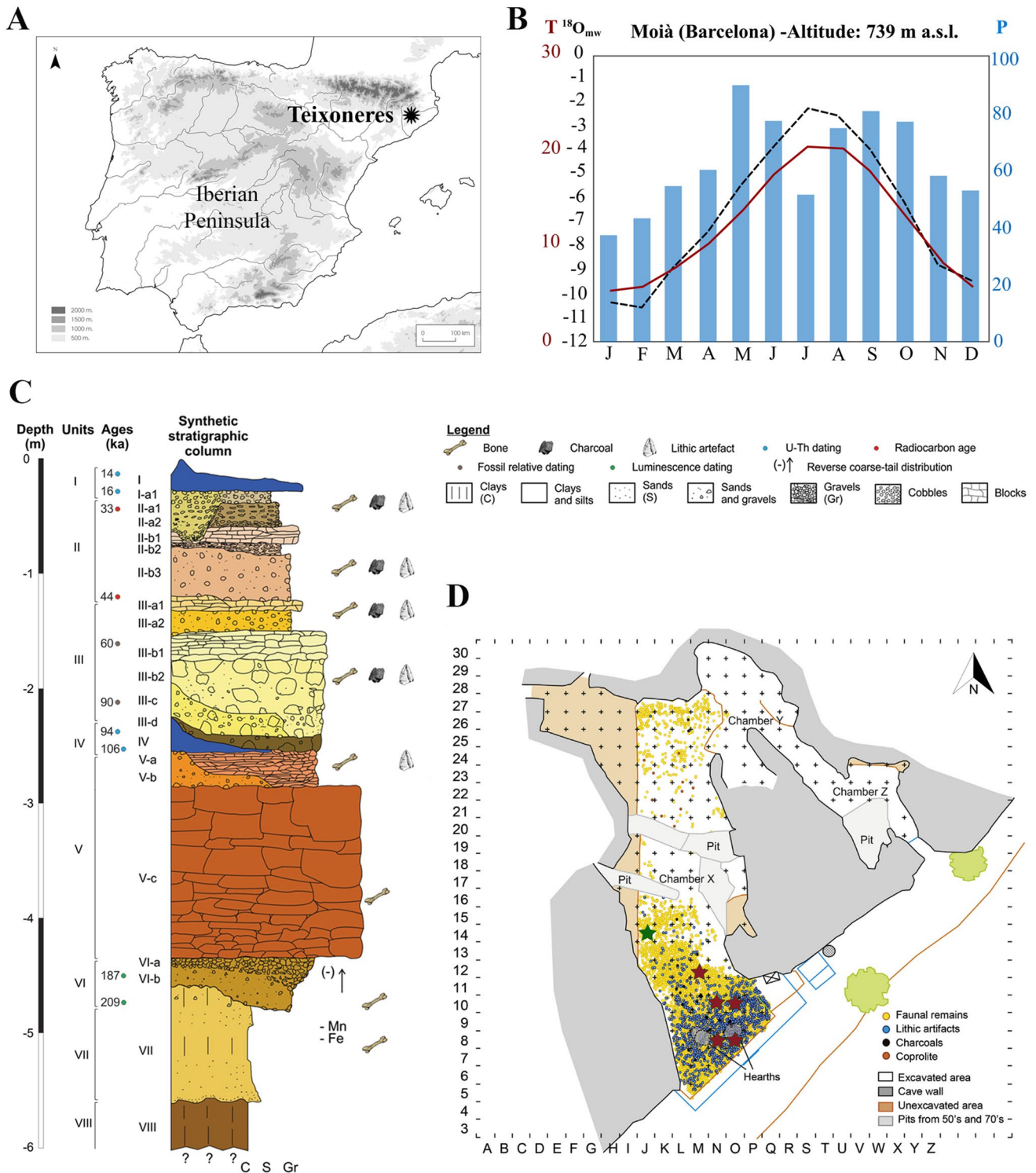


**Fig. 1** A Location of the Teixoneres Cave in Iberia; B current monthly temperatures (continuous line; T; in °C) and precipitations (bars; P; in mm) (Climate-data.org) and present-day oxygen isotope composition of meteoric waters (dash black;  $\delta^{18}O_{mw}$  2017) of Moia; C synthetic stratigraphic sequence of chamber X in Teixoneres Cave, modified from Zilio et al. (2021); U-Th series (Tissoux et al. 2006)

and radiocarbon dates (Talamo et al. 2016); D ground plan of unit III of Teixoneres Cave showing the 3D-position of the recovered items: lithics (blue), faunal remains (yellow), charcoals (black), and coprolites (brown). Squares sampled for taphonomic analyses of small mammals correspond to red (unit III) and green (unit II) stars. Drawing modified from Rosell et al. (2017)



Pleistocene palaeontological record. Since 2003, systematic excavations are annually undergone under the leadership of a multidisciplinary team of the *Institut Català de Paleoeologia Humana i Evolució Social* (IPHES) excavating in extension the whole surface of the Teixoneres Cave, ~250 m<sup>2</sup> (Rosell et al. 2008, 2010a, b, 2014).

Teixoneres Cave is composed of three main chambers (X, Y, and Z) that together form a 30 m length U-shape, with two access points from chambers X and Z (Fig. 1D). Chamber X is the biggest gallery, which is 30-m-long and filled with a 6-m-thick sediment package containing eight archaeopalaeontological units, including two speleothems (unit I and IV) (Rosell et al. 2008, 2010a; Zilio et al. 2021). The dates of unit I (ca. 14–16 ka) and unit IV (ca. 100.3 ± 6.1 ka) have been obtained through U-series dating of stalagmite layers (Fig. 1C) (Tissoux et al. 2006). More recently, radiocarbon dates adjusted the chronology of unit III, from > 51,000 <sup>14</sup>C BP to 44,210 cal BP, and unit II, which extends from 44,210 to 33,060 cal BP (Talamo et al. 2016). This work focuses on these two units (II and III) of Chamber X, which have been the focus of recent excavations (Rosell et al. 2008, 2010b; Rufà et al. 2016). Both are units comprising sandy lutites and limestone blocks. A distinction between two archaeostratigraphic subunits (IIa and IIb) has been drawn due to the presence of large limestone blocks at the base of IIa. In turn, at least two different subunits (IIIa and IIIb) can be appreciated in unit III, distinguished by an increased presence of reddish clays in IIIb, limestone blocks at the base of IIIa, and the increased abundance of archaeological material in IIIb. The sediment comes from allochthonous colluvial clays and silts, which entered the cave through the main entrance and a chimney located on the northeast side of the cave. Those sediments imbricate at the center of the main gallery. An autochthonous component is formed by limestone blocks falling from the walls and the roof of the cave.

Most previous studies concluded that there were short-term human occupations of the cave, in alternance with use by carnivorous predators, ruling out temporal contact between them (Rosell et al. 2010a, b, 2014, 2017; Rufà et al. 2014, 2016; Sánchez-Hernández et al. 2014, 2016; Bustos-Pérez et al. 2017; Picin et al. 2020; Zilio et al. 2021). Moreover, a bimodal spatial distribution is observed, of which human groups tend to concentrate their activities at the entrance of the cave, whereas carnivores and other predators preferentially use the inner areas (Fig. 1D). Among large mammals, a wide diversity of species was recorded in the cave, where both ungulates (*Equus ferus*, *Equus hydruntinus*, *Cervus elaphus*, *Capreolus capreolus*, *Bos primigenius*, *Sus scrofa*, *Capra pyrenaica*, and *Rupicapra pyrenaica*) and carnivores (*Ursus spelaeus*, *Crocota crocuta*, *Canis lupus*, *Vulpes vulpes*, *Lynx spelaea*, *Meles meles*) are frequent. Medium-sized vertebrates were also identified as tortoise (*Testudo hermanni*), leporids (*Oryctolagus cuniculus* and

*Lepus* sp.), and birds (Corvidae, Phasianidae, Strigidae and Columbidae) (Rosell et al. 2008, 2010a, b; Rufà et al. 2014, 2016). The presence of two cold-adapted species has also been recorded, *Mammuthus primigenius* and *Coelodonta antiquitatis* (Álvarez-Lao et al. 2017). Both hominin and carnivore activities were documented among larger fauna. Human butchering activities, mainly concerning ungulates, were confirmed from the detection of cut marks, fresh fractures, and burning (Rosell et al. 2008, 2010a, b). Analyzed leporid and bird remains are not primarily related to human activity, but with mammalian carnivores and raptors inputs (Rufà et al. 2014, 2016). However, sporadic consumption of leporids by humans was detected. The presence of Neanderthal groups is confirmed at the site by the discovery of Mousterian lithic tools. Raw materials have a local or semi-local origin (< 15 km) and consist mainly of quartz, followed by chert, agates, and limestones. Reduction sequences are highly fragmented, consisting in flakes and final products, with some retouched tools (mainly scrapers) and in subunit IIIb also bone retouchers, linked to the short-term occupation patterns (Rosell et al. 2010a, b; Talamo et al. 2016; Bustos-Pérez et al. 2017; Mateo-Lomba et al. 2019). In unit III, Picin et al. (2020) proposed a differentiation between in situ knapping activities in local quartz and the mobile toolkit transported at the site. It was thus interpreted as a combination of hunting tools and cutting artefacts used during the primary butchery of the hunted preys in their punctuated visits to the cave. Some combustion structures characterized by sediment areas with rubefaction or hearths were mainly detected at the entrance in unit III (Rosell et al. 2010b, 2014). Moreover, human remains are represented by three deciduous teeth corresponding to at least two different individuals younger than 7 years old along with a molar of an adult.

### Environmental context: past and present

The Moià region is nowadays included in the continental Mediterranean climate, at the boundary between the humid and sub-humid areas inside the Catalanian climatic subdivisions (Servei Meteorològic de Catalunya 2018), near the boundary of the Mediterranean and Eurosiberian regions. The climate is generally wet and temperate (mean annual temperatures around 12 °C), but with hot summers (18–21 °C) and cold winters (5–6 °C), along with a consequent thermic annual oscillation around 15 °C. Mean annual rainfall is 700–800 mm. Precipitation is abundant throughout the year, with autumn and spring being the wettest periods and winters being slightly drier (Climate-data.org 2018; Servei Meteorològic de Catalunya 2018). There is consistent correspondence between average monthly temperatures and monthly oxygen isotope compositions of meteoric water estimated for the area (OIPC data; Bowen 2017; Climate-Data.

org 2018) (Fig. 1B). The area is in the supramediterranean belt (Rivas-Martínez 1987; Rivas-Martínez et al. 2007), dominated by forests (mainly box, pine, and oak) adapted to mild summers and cold winters (Ochando et al. 2020).

Different approaches to reconstruct the palaeoecological conditions of Teixoneres Cave were performed. The specific attribution of the small-vertebrate remains (amphibians, squamates reptiles, and small mammals) was performed by López-García et al. (2012a, b, 2014). Small-vertebrate assemblage abundances underline a clear predominance of forest components (> 60%), especially in unit III, with some faunal component changes between Mediterranean and Mid-European taxa, from base to top. These data, in combination with pollen, charcoal, and large-mammal dental wear analyses, describe an open forest landscape, with temperate and humid conditions during the formation of unit III, and cooler and drier conditions during the formation of unit II (López-García et al. 2012a; Sánchez-Hernández et al. 2016, 2020a, b). Palynological data confirm a landscape dominated by woodlands composed of pines and oaks and some open areas (herbaceous taxa such as *Poaceae*, *Chenopodiaceae*, and *Astareceae*), always showing high proportions of arboreal pollen (> 50%). The most recent and complete palynological study (Ochando et al. 2020) described a mixed oak-pine forest with a high diversity of woody taxa that combines evergreen trees (*Quercus*), deciduous trees (*Quercus suber*; *Juniperus*), and the occurrence of *Corylus*, *Castanea*, *Betula*, *Fraxinus*, *Buxus*, *Olea*, *Populus*, *Salix*, *Abies*, *Taxus*, *Cedrus*, *Acer*, *Alnus*, *Celtis*, *Juglans*, *Fagus*, *Ulmus*, *Calicotome*, *Ceratonia*, *Cistus*, *Ephedra fragilis*, *Myrtus*, *Pistacia*, *Phillyrea*, *Rhamnus*, and *Viburnum*. Notably, high peaks of oak pollen are noticed in units III to I. Charcoal remains are scarce in the cave, but four taxa are recorded (*Buxus sempervirens*, *Pinus pinea/pinaster* type, *Pinus sylvestris* type, and *Quercus* sp.) (López-García et al. 2012a). The morphometric variation of the first lower molars of two vole species abundant at the site, *Microtus agrestis* and *Microtus arvalis*, indicates that the former decreased from subunit IIIa to IIb. In contrast, *M. arvalis* increased from IIIa to IIb (Luzi et al. 2017). The authors related these changes to better water management given the decrease in humidity from lower to upper units.

## Materials and methods

### Taphonomic analysis

The small-mammal remains included in this analysis consist mainly of isolated teeth and bones recovered from sediment samplings (organized in 5–10 cm splits) from the entire excavated surface of Chamber X (divided in 1 × 1 m), completed during excavation seasons from 2008 to 2016.

The remains were collected by washing and sieving the sediment, with two superimposed meshes of 5 mm and 0.5 mm, and selected by subsequent sorting. Remains were observed under light microscopes (Exacta-Optech LFZ 10x-90x; Olympus SZ-PT 18x-50x). Due to the high amount of small-mammal material available at the site, specific squares were selected for the taphonomic analysis by considering the subunit divisions (IIIb, IIIa, IIb, IIa) to evaluate potential taphonomical difference between these subunits (Fig. 1D). For unit II, square J14 was selected, which is the site area with the most abundant small-mammal remains. Not enough material was available in unit III from this square, and a random selection including squares N8, O8, N10, O10, and M12 was chosen from the exterior part of the cave, where the human occupations were more intense.

The identified remains were counted (NISP) and grouped using the minimum number of individuals (MNI) method, determined by counting the most highly represented diagnostic element, considering laterality. Dental remains were considered independently whether they are in situ or isolated (e.g. each molar on a mandible is counted as a single remain). The MNI was adapted according to the taphonomic sampling performed by considering the minimum number of elements (MNE) of each subunit. The taphonomic study was based on the observation and description of the superficial modifications of skeletal elements (Andrews 1990; Fernández-Jalvo and Andrews 2016; Fernández-Jalvo et al. 2016) including the differentiation between predation and post-depositional damage. The taphonomic analysis included all rodent elements in anatomical representation (recount and indexes explanation detailed in Appendix 1) and incisors, molars, femora, and humeri of rodents were included in analyses of breakage, digestion, and post-depositional modifications. The analyses of soricids, talpids, and chiropters were also considered in the final interpretation.

### Oxygen isotope analysis

Oxygen isotope compositions ( $\delta^{18}\text{O}$ ) were measured on 40 rodent teeth from subunits IIIb, IIIa, IIb, and IIa. To avoid possible interspecific variability, *Apodemus sylvaticus* fossil lower incisors were preferentially selected, with thirty-four incisors corresponding to at least twenty-two individuals (Table 1). However, well-preserved incisors were not always available, and so, four teeth of the subfamily Arvicolinae in subunit IIb ( $n=1$ ) and IIa ( $n=3$ ) and two teeth of the species *Eliomys quercinus* in subunit IIIb and IIa were also included. In total, ten samples from each subunit were selected in order to gather a representative range of samples (Lindars et al. 2001; Gehler et al. 2012; Royer et al. 2013b; Peneycad et al. 2019). Oxygen isotope analysis performed on present-day material coming from the Moia area is also included. The remains came from one pellet recovered at the end of

**Table 1** Oxygen isotope composition of tooth enamel phosphate ( $\delta^{18}\text{O}_p$ ; ‰ V-SMOW) from rodent lower incisors from Teixoneres Cave. The table includes the stratigraphic, identified taxa, and the conversion to the oxygen isotope composition of meteoric waters ( $\delta^{18}\text{O}_{mw}$ ; ‰ V-SMOW) following the Royer et al. (2013a) oxygen isotope fractionation equation. *SD* standard deviation

Sample	Subunit	Taxon	Laterality	Location	$\delta^{18}\text{O}_p$ (‰ V-SMOW)	SD	$\delta^{18}\text{O}_{mw}$ (‰ V-SMOW)
TX430	IIa	Arvicolinae	Right	Isolated	20.4	0.2	-3.6
TX431	IIa	<i>Apodemus cf. sylvaticus</i>	Right	Isolated	19.0	0.2	-4.8
TX429	IIa	<i>Apodemus cf. sylvaticus</i>	Left	Isolated	18.9	0.1	-4.9
TX433	IIa	Arvicolinae	Left	In situ	18.8	0.3	-4.9
TX432	IIa	<i>Apodemus cf. sylvaticus</i>	Right	Isolated	18.7	0.4	-5.0
TX355	IIa	<i>Apodemus cf. sylvaticus</i>	Left	Isolated	18.2	0.5	-5.4
TX348	IIa	<i>Eliomys quercinus</i>	Left	In situ	18.0	0.3	-5.6
TX164	IIa	<i>Apodemus cf. sylvaticus</i>	Right	Isolated	17.8	0.4	-5.7
TX163	IIa	<i>Apodemus cf. sylvaticus</i>	Left	Isolated	17.3	0.3	-6.2
TX356	IIa	Arvicolinae	Left	Isolated	16.6	0.3	-6.7
TXB161	IIb	<i>Apodemus cf. sylvaticus</i>	Left	Isolated	20.3	0.2	-3.7
TXB160	IIb	Arvicolinae	Right	Isolated	19.3	0.4	-4.5
TXB377	IIb	<i>Apodemus cf. sylvaticus</i>	Right	Isolated	19.3	0.3	-4.5
TXB385	IIb	<i>Apodemus cf. sylvaticus</i>	Left	Isolated	19.2	0.3	-4.6
TXB381	IIb	<i>Apodemus sylvaticus</i>	Right	In situ	18.3	0.2	-5.3
TXB387	IIb	<i>Apodemus cf. sylvaticus</i>	Left	In situ	18.1	0.1	-5.5
TXB383	IIb	<i>Apodemus cf. sylvaticus</i>	Right	Isolated	18.0	0.3	-5.6
TXB378	IIb	<i>Apodemus cf. sylvaticus</i>	Left	Isolated	18.0	0.5	-5.6
TXB382	IIb	<i>Apodemus cf. sylvaticus</i>	Left	Isolated	17.9	0.3	-5.7
TXB376	IIb	<i>Apodemus cf. sylvaticus</i>	Left	Isolated	16.8	0.3	-6.6
TX3816	IIIa	<i>Apodemus cf. sylvaticus</i>	Left	In situ	19.5	0.2	-4.3
TX3814	IIIa	<i>Apodemus cf. sylvaticus</i>	Right	Isolated	19.1	0.3	-4.7
TX3145	IIIa	<i>Apodemus cf. sylvaticus</i>	Right	Isolated	18.7	0.4	-5.0
TX3813	IIIa	<i>Apodemus cf. sylvaticus</i>	Left	In situ	18.3	0.2	-5.4
TX3815	IIIa	<i>Apodemus cf. sylvaticus</i>	Right	In situ	18.1	0.2	-5.5
TX38111	IIIa	<i>Apodemus sylvaticus</i>	Right	In situ	17.7	0.3	-5.9
TX3820	IIIa	<i>Apodemus cf. sylvaticus</i>	Right	In situ	16.7	0.3	-6.7
TX3819	IIIa	<i>Apodemus cf. sylvaticus</i>	Right	Isolated	16.7	0.3	-6.7
TX3818	IIIa	<i>Apodemus cf. sylvaticus</i>	Right	In situ	16.5	0.3	-6.8
TX3823	IIIa	<i>Apodemus cf. sylvaticus</i>	Right	Isolated	15.5	0.3	-7.7
T3B525	IIIb	<i>Apodemus cf. sylvaticus</i>	Right	Isolated	21.3	0.4	-2.9
T3B1000	IIIb	<i>Apodemus sylvaticus</i>	Left	In situ	20.3	0.3	-3.7
T3B421	IIIb	<i>Apodemus sylvaticus</i>	Left	In situ	18.9	0.2	-4.8
T3B424	IIIb	<i>Apodemus cf. sylvaticus</i>	Right	Isolated	18.6	0.5	-5.1
T3B524	IIIb	<i>Eliomys cf. quercinus</i>	Left	In situ	18.2	0.4	-5.5
T3B423	IIIb	<i>Apodemus cf. sylvaticus</i>	Left	Isolated	17.7	0.5	-5.8
T3B432	IIIb	<i>Apodemus sylvaticus</i>	Left	In situ	17.6	0.5	-6.0
T3B435	IIIb	<i>Apodemus sylvaticus</i>	Left	In situ	17.4	0.4	-6.1
T3B492	IIIb	<i>Apodemus sylvaticus</i>	Right	In situ	16.1	0.3	-7.1
T3B2000	IIIb	<i>Apodemus cf. sylvaticus</i>	Right	Isolated	16.0	0.4	-7.2

August from a barn owl (*Tyto alba*) nest, located at 7.7 km from Teixoneres Cave at 1000 m a.s.l (Table 2; Fernández-García et al. 2019). These remains consist of three lower incisors from *M. (T.) duodecimcostatus* and *M. musculus*. One extra lower incisor of *M. (T.) duodecimcostatus* was also included from scattered pellets on the nest. The season in which this last element was produced is unknown.

The wet chemistry and the mass spectrometer measurements were developed in the Laboratoire de Géologie of Université Claude Bernard (Lyon, France). The rodent teeth were ultrasonicated and enamel fragments were selected by hand-picking and the basal part of the enamel was discarded. Enamel was homogenized by crushing in an agate mortar. The enamel tooth samples were treated following the wet

**Table 2** Oxygen isotope composition of tooth enamel phosphate ( $\delta^{18}\text{O}_p$ ; ‰ V-SMOW) from rodent lower incisors from modern pellets of Moia. The table includes the provenance of remains, identified

taxa, and the conversion to the oxygen isotope composition of meteoric waters ( $\delta^{18}\text{O}_{mw}$ ; ‰ V-SMOW) following the Royer et al. (2013a) oxygen isotope fractionation equation. *SD* standard deviation

	MA-12	MA-4	MA-6	MA-5
Origin	Scattered pellets	Pellet	Pellet	Pellet
State	Disaggregated	Semi-dry	Semi-dry	Semi-dry
Recovering	Unknown	End of August	End of August	End of August
Taxon	<i>M. (T.) duodecimcostatus</i>	<i>M. (T.) duodecimcostatus</i>	<i>M. musculus</i>	<i>M. musculus</i>
Laterality	Right	Left	Right	Left
$\delta^{18}\text{O}_p$ (‰ V-SMOW)	16.1	18.6	19.2	19.5
SD	0.4	0.4	0.3	0.3
$\delta^{18}\text{O}_{mw}$ (‰ V-SMOW)	-7.2	-5.1	-4.6	-4.4

chemistry procedure described by Crowson et al. (1991) and Lécuyer et al. (1993), adapted for small-sample weights (Bernard et al. 2009). This protocol is based on the isolation of phosphate ions ( $\text{PO}_4^{3-}$ ) from apatite as silver phosphate ( $\text{Ag}_3\text{PO}_4$ ) crystals using acid dissolution and anion-exchange resin. For each sample, around 1–3 mg of enamel powder was dissolved in 1 ml 2 M HF overnight.  $\text{CaF}_2$  residue was isolated by centrifugation and the solution was neutralized by adding 1 ml 2 M KOH; then 1.5 ml of Amberlite™ anion-exchange resin was added to separate the  $\text{PO}_4^{3-}$  ions. After 24 h, the solution was removed, and phosphate was eluted from the resin with 6 ml 0.1 M  $\text{NH}_4\text{NO}_3$ . After 4 h, 0.1 ml  $\text{NH}_4\text{OH}$  and 3 ml of  $\text{AgNO}_3$  were added to the solution and the samples were placed in a thermostatic bath at 70 °C for 6 h, enabling the precipitation of  $\text{Ag}_3\text{PO}_4$  crystals. Four standard samples of natural phosphorite (NBS120c) were included during each batch of wet chemistry. Oxygen isotope compositions were measured using a varioPYROcube™ elemental analyser interfaced in continuous flow mode with an isotopic ratio mass spectrometer Isoprime™ (EA-Py-CF-IRMS technique performed at CNRS UMR 5276 LGL; Lécuyer et al. 2007; Fourel et al. 2011). Measurements were calibrated with the standard samples of NBS120c phosphorite (21.7‰; V-SMOW; Lécuyer et al. 1993), and NBS127 barium sulfate (9.3‰; V-SMOW; Hut 1987). Samples were measured usually in five replicates, but in some cases just three. Based on phosphate chemical yields measured during the wet chemistry procedure, clustered phosphorus pentoxide ( $\text{P}_2\text{O}_5$ ) contents close to 35 wt% indicate that the original stoichiometry of the teeth was most likely preserved (Navarro et al. 2004; Héran et al. 2010; Royer et al. 2013a). The average standard deviation of  $\delta^{18}\text{O}$  for the Teixoneres samples is  $0.31 \pm 0.03\%$  ( $n = 40$ ) and NBS120c quality control standards included in precipitation provide  $21.5 \pm 0.3\%$  ( $n = 16$ ), homogenous results close to their consensus value.

### Palaeotemperature estimations

Usually, air temperatures are estimated from  $\delta^{18}\text{O}_p$  by a two-step procedure involving two linear equations: (1) the measured  $\delta^{18}\text{O}_p$  values of the fossil rodent teeth allow for the estimation of the  $\delta^{18}\text{O}$  values of local meteoric water ( $\delta^{18}\text{O}_{mw}$ ), and (2) the calculated  $\delta^{18}\text{O}_{mw}$  values can be used to estimate past air temperatures. This method assumes that temperature is the dominant factor controlling the  $\delta^{18}\text{O}_{mw}$  values recorded at mid- and high latitudes (Dansgaard 1964; Rozanski et al. 1993). However, secondary effects such as latitude, distance to sea, altitude, and distinct humid air mass trajectories in the past should also be considered. In parallel, oxygen isotope compositions of vertebrate biogenic apatite phosphate are linearly correlated to the oxygen isotope composition of their environmental waters (e.g., Longinelli 1984; Luz et al. 1984), with the physiology of each species being recorded in the oxygen isotope fractionation equation empirically established by the use of present-day individuals.

In this work, mean annual temperatures (MAT) were calculated from  $\delta^{18}\text{O}$  analysis of each subunit, following the strategy proposed for  $\delta^{18}\text{O}_p$  from rodent teeth accumulated in the Iberian Peninsula (Fernández-García et al. 2019), that employed: (1) the empirically determined oxygen isotope fractionation equation established for extant rodent species for transforming  $\delta^{18}\text{O}_p$  into  $\delta^{18}\text{O}_{mw}$  [Royer et al. 2013a:  $\delta^{18}\text{O}_p = 1.21 (\pm 0.20) \times \delta^{18}\text{O}_{mw} + 24.76 (\pm 2.70)$ ]; and (2) a linear regression model relating  $\delta^{18}\text{O}_{mw}$  and air temperatures based in IAEA Iberian stations climatic records [MAT (°C) =  $2.388 (\pm 0.10) \times \delta^{18}\text{O}_{mw} + 28.19 (\pm 0.58)$ ]. Indeed, this proposal takes into account the possible temperature seasonal bias derived from a preferent spring–summer rodent accumulation by predation [Fernández-García et al. 2019, 2020:  $\delta^{18}\text{O}_{mw}$  (annual mean) =  $1.04 (\pm 0.05) \times \delta^{18}\text{O}_{mw}$  (March–June



mean)—0.86( $\pm 0.28$ )] and also corrected the ice-sea level fluctuations that impact the  $\delta^{18}\text{O}$  of seawater (Schrag et al. 2002), which is the source of humid air masses (estimated in  $+0.6\text{‰}$  for MIS 3 sea level descent).

In parallel, MAT and precipitations (mean annual precipitations; MAP) are compared with two qualitative and independent palaeoenvironmental methods: the mutual eco-geographic range (MER) and the bioclimatic model (BM) (detailed explanation in Appendixes 3 and 4). The former was previously calculated for the Teixoneres site by López-García et al. (2012a, b, 2014), but this work applies the BM method for the first time (Hernández Fernández 2001; Hernández Fernández et al. 2007; Royer et al. 2020). The current temperature data recorded in the Teixoneres area (Moià) are taken from Climate-Data.org (<https://es.climate-data.org/>). Present-day  $\delta^{18}\text{O}_{\text{mww}}$  values for the Teixoneres area were obtained using the Online Isotopes in Precipitation Calculator (OIPC; Bowen 2017) based on datasets collected by the Global Network for Isotopes in Precipitation (IAEA/WMO, 2018).

## Results and discussion

### Origin of small mammals

The taphonomic analysis was completed on 2642 remains (Table 3; Figs. 2 and 3). The most frequent taxonomic group is the order Rodentia (NISP = 1536; 58.0%), followed by chiropters (NISP = 163; 6.0%), talpids (NISP = 11; 0.5%), and soricids (NISP = 37; 1.4%) in lower proportions (Appendix 1). Higher relative abundances of skeleton elements have been recorded in unit III (around 55%) than in unit II (IIb = 29%; IIa = 42%). However, all subunits shared a similar pattern regarding the skeletal part conservation. According to indexes comparing cranial and postcranial elements, these are almost in equilibrium, but slightly better preservation of dental elements (molars and, especially, incisors) is noticed, except for subunit IIa (Table 3). A preferential destruction of distal over proximal extremities is noticed. Breakage of mandibles and maxillae can be deduced, especially for lower subunits. Most recovered teeth in these assemblages are isolated ( $>90\%$  of incisors and  $>75\%$  of molars). Molar breakage is low, around 15–20% in subunits IIIb and IIb, and 8–10% in subunits IIIa and IIa. On the contrary, total breakage in incisors is around 65% for unit III and around 45% for unit II. All humeri and femora found in the sample were broken.

Digestion percentages ranged between 31% in subunit IIb and 43% in subunit IIa; subunits IIIb and IIIa had an almost equal proportion of total digested elements (Table 3; Fig. 2). Different degrees of digestion are observed from light to heavy, except for subunit IIIb where extreme degrees are

also detected. At least 35% of the elements in unit III exhibit digestion marks, which show a practically equal pattern in the digestion of incisors (50%) and molars (around 25%). Unit II is not far from these estimations, but there is a certain disturbance within their subunits, as both present an equivalent number of digested molars and incisors: around 30% in subunit IIb and around 40% in subunit IIa. Postcranial digestion accounts for around 40% of the elements, except for subunit IIIb ( $<30\%$ ). Occasionally, intra-mandibular digestion of incisors was identified in all subunits. Digestion was occasionally detected in bats (subunit IIb and IIIb) and also in soricids (IIIb), for which extreme degrees of digestion are reached. Bat remains were preliminarily considered a result of both predation and in situ death, because the species has been recorded to frequently inhabit caves (Kowalski 1995; Palomo et al. 2007; López-García et al. 2012a).

More than 30% of elements in each subunit were affected by digestion, and skeleton parts spectra are fragmentary, confirming that predation was the main cause of small-mammal accumulation. Breakage and proportional representation indexes are not coincident with any predator pattern (Andrews 1990), even sometimes showing values included in Categories 4 and 5 of predators. It is common for indexes in archaeological contexts to differ from those of modern collections, because palimpsests and long-term post-depositional processes can occur. The predominance of remains without digestion marks, light alterations being the most frequent degree of digestion, low frequency of heavy digestions, and the absence of extreme digestion (except in subunit IIIb) throughout the sequence point to nocturnal raptors as the main agent. They do not support the possibility of intervention by predators included in Categories 4–5 (Andrews 1990), such as diurnal raptors or small carnivores, as the observed fragmentation rates could initially suggest (Andrews 1990; Fernández-Jalvo and Andrews 1992; Terry 2007; Lloveras et al. 2008a, b, 2012; Comay and Dayan 2018). The occasional extreme digestions recorded in subunit IIIb (2% of rodents, but also detected in some *Soricidae* remains) can be consistent either with unfrequented damage inflicted by owls related to different physiological or ethological factors (Andrews 1990; Royer et al. 2019) or most likely consequence of the punctual intervention of small carnivores in the cave.

Globally, the progressive proportion of degrees of digestion across each anatomical element and the correlation between proportion and degrees of digestion between the analyzed skeleton elements could indicate that a single type of predator is the most likely cause (Bennàsar 2010; Bennàsar et al. 2016). The fraction of digestion remains, and the degree of digestion attained, besides medium–high relative abundance of elements and molar breakage recorded by small mammals analyzed at all subunits, fits with an intermediate modification predator (Andrews 1990), such

**Table 3** Summary of taphonomic variables analyzed, including recounts (*NR* number of remains; *NISP* number of identified specimens; *MNI* minimum number of individuals of order Rodentia considered in skeletal representation), alterations caused by predation (skeletal representation, proportional representation indexes, breakage, and digestion), and post-depositional alterations

	IIIb		IIIa		IIb		IIa	
<b>Recount</b>								
NR ( <i>n</i> )	782		988		388		484	
NISP ( <i>n</i> )	573		791		323		402	
Rodent MNI ( <i>n</i> )	22		31		23		22	
<b>Skeletal representation</b>								
Relative Abundance Index (%)	58.5		62.1		33.6		47	
SD of Relative Abundance Index	42.2		42.2		14.9		47	
<b>Proportional representation indexes</b>								
Postcranial/Cranial Index	46.8		47.6		45.7		78.8	
Humerus + Femur/Maxilla + Mandible Index	54.0		51.6		49.3		55.4	
Radius + Tibia/Humerus + Femur Index	40.5		35.2		33.3		31.3	
Isolated teeth/Empty Alveolus Index	67.2		74.8		60.6		54.8	
<b>Breakage</b>								
Incisors fracture (%)	68.1		68		45.8		42	
Molars fracture (%)	11.7		8.3		17.1		6.9	
Postcranial fracture (%)	100		100		100		100	
<b>Digestion</b>								
	<i>n</i>	%	<i>n</i>	%	<i>n</i>	%	<i>n</i>	%
<b>Total digested elements</b>								
<i>Light degree</i>	63	24.1	105	28.5	36	23.5	56	31.1
<i>Moderate degree</i>	17	7	22	6	10	7	15	8
<i>Heavy degree</i>	9	3.4	7	1.9	2	1.3	7	3.9
<i>Extreme degree</i>	4	2	0	0	0	0	0	0
<b>Digested incisors</b>								
<i>Light degree</i>	32	32.3	61	40.1	11	21.6	14	29.2
<i>Moderate degree</i>	12	12.1	13	8.6	3	5.9	5	10.4
<i>Heavy degree</i>	3	3	2	1.3	2	3.9	2	4.2
<i>Extreme degree</i>	2	2	0	0	0	0	0	0
<b>Digested molars</b>								
<i>Light degree</i>	25	18.7	29	16.8	16	20.5	29	29.3
<i>Moderate degree</i>	3	2.2	5	2.9	7	9	10	10.1
<i>Heavy degree</i>	6	4	5	3	0	0	5	5
<i>Extreme degree</i>	2	1	0	0	0	0	0	0
<b>Digested postcrania</b>								
<i>Light degree</i>	6	21.4	15	34.1	9	37.5	13	39.4
<i>Moderate degree</i>	2	7.1	4	9.1	0	0	0	0
<i>Heavy degree</i>	0	0	0	0	0	0	0	0
<i>Extreme degree</i>	0	0	0	0	0	0	0	0
<b>Post-depositional agents</b>								
	<i>n</i>	%	<i>n</i>	%	<i>n</i>	%	<i>n</i>	%
<b>Striations</b>								
	295	79.1	381	79	167	79.5	171	77.4
<b>Fissures</b>								
	104	27.9	141	29.3	34	16.2	46	20.8
<b>Cracks</b>								
	33	8.8	56	11.6	10	4.8	4	1.8
<b>Cementation</b>								
	20	5.4	57	11.8	2	1	3	1.4
<b>Manganese oxide pigmentation</b>								
	175	46.9	177	36.7	121	57.6	108	48.9
<b>Chemical corrosion—plant activity</b>								
	126	33.8	105	21.8	34	16.2	35	15.8
<b>Burning</b>								
	7	1.9	2	0.4	2	1	0	0

Bold is used to mark the main indexes and alterations considered in the analysis

as *Bubo bubo* or *Strix aluco*. Distinguishing between these two owls is not simple, as both inflict similar damages on small-mammal remains. Subunits IIIa and IIIb, which

provide similar digestion patterns in each skeletal element, present some characteristics more consistent with patterns expected from *B. bubo* than those from *S. aluco* (Andrews

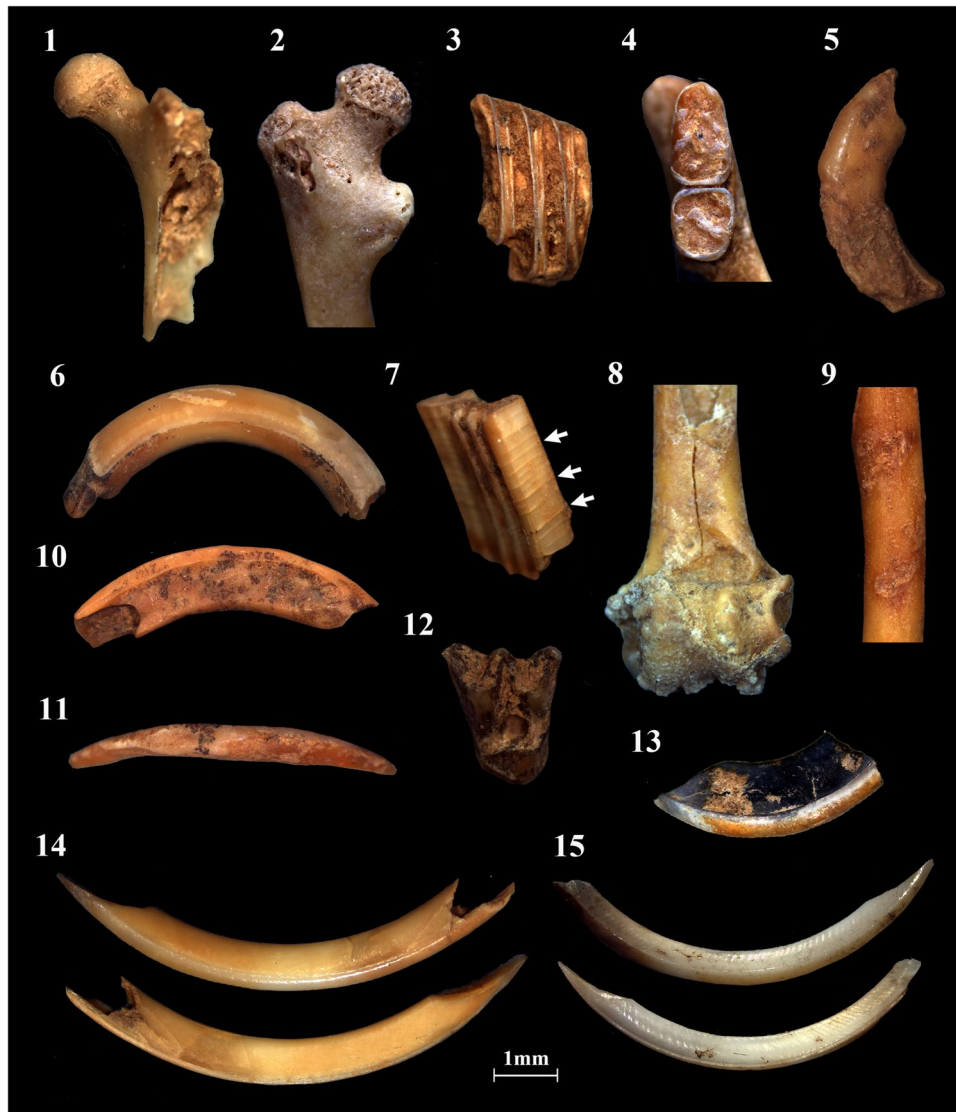


**Fig. 2** Some taphonomic features detected on small-mammal remains from Teixoneres Cave and oxygen isotope samples. (1) Left femur proximal epiphysis of a rodent with light digestion (subunit IIIa); (2) left femur proximal epiphysis of a rodent with moderate digestion (IIIa); (3) Arvicolinae molar with heavy digestion (IIIa), in lateral view; (4) right first and second lower molars of *Apodemus sylvaticus* with extreme digestion (IIIb), in occlusal view; (5) rodent upper incisor with light digestion (on the tip) and root damage (on the posterior part) (IIIa), in lateral view; (6) rodent upper incisor with light intramandibular digestion, with scattered manganese oxide pigmentation on dentine and root imprints in enamel (IIIa); (7) Arvicolinae molar

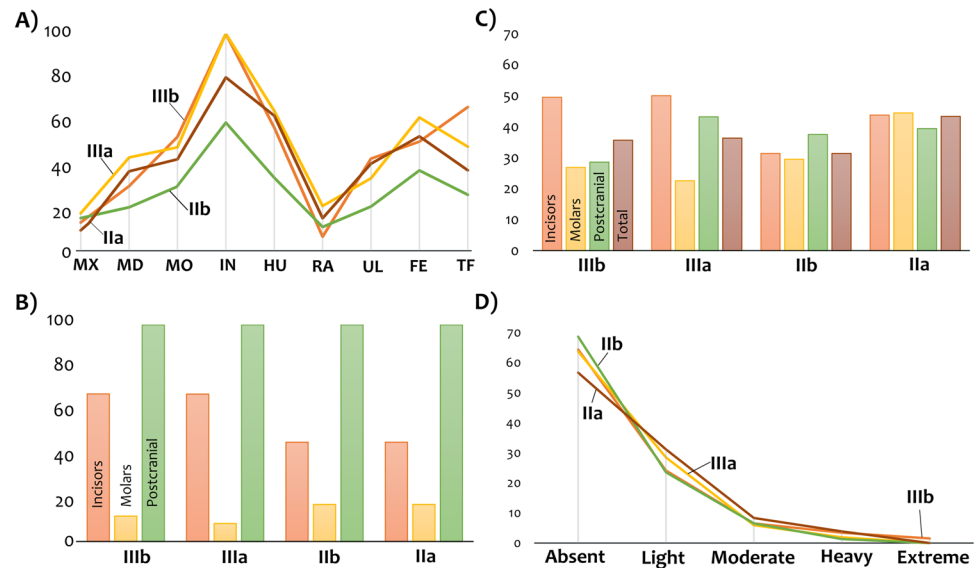
with fissures related to humidity changes (IIIa); (8) right humerus distal epiphysis of *Myotis myotis-blythii* with cementation (IIIb); (9) roots imprints on a rodent femur shaft (IIIb); (10) rodent upper incisor with extreme digestion (IIIb), in lateral view; (11) rodent lower incisor with heavy (IIIb), in occlusal view; (12) right upper molar of *Myotis myotis-blythii* with widespread manganese oxide pigmentation (IIIa), in occlusal view; (13) burned rodent upper incisor (IIIa), in lateral view; (14) left lower incisor fossil of *Apodemus sylvaticus* (level IIIa), in labial and lingual view; (15) modern right lower incisor modern of *Mus musculus* (origin: *Tyto alba* pellet), in labial and lingual view. (14) and (15) are included in biochemical analysis. Scale 1 mm

1990; Fernández-Jalvo 1992; Bennàsar et al. 2016; Lebreton et al. 2020). This owl tends to produce higher relative abundances of elements (around 60%), a low incidence of heavy digestion, while it introduces in its diet medium-sized preys such as leporids (some of which have been already related to this predator in unit III, Rufà et al. 2014). Digestion patterns moreover are highly in agreement with those reported

for *B. bubo* by Lebreton et al. (2020) and those summarized by Fernández-Jalvo et al. (2016).

This pattern is clear for unit III, but less so for unit II, for which some clarifications should be made. Considering the scarcity of remains with moderate and heavy digestion and the absence of tooth marks, diurnal raptors and carnivores can be ruled out as the main cause (Andrews 1990). Thus, the main action of a predator of intermediate modification

**Fig. 3** Taphonomic variables related to predation observed on rodents from subunits IIIb–IIa. **A** Skeletal profile based on relative abundances of maxillae (MX), mandibles (MD), molars (MO), incisors (IN), humeri (HU), radii (RA), ulnae (UL), femora (FE), and tibia-fibula (TF); **B** breakage rates; **C** digestion percentages; **D** total degree reached



can be confirmed, but considering present-day reference collections (Andrews 1990; Fernández-Jalvo et al. 2016), none of the nocturnal birds of prey inflicted equal damage to molars and incisors. The presence of this equal damage in these subunits is most likely attributed to a combination of different groups of owls, which produce low to intermediate modifications. It is possible that *B. bubo* continued to contribute to unit II, but other predator inputs obscure the results. In addition, the low quantity of remains involved in the analysis of these subunits and the higher presence of the Arvicolinae subfamily should also be considered. The enlarged sample presented in this work provides enough remains to rule out the preliminary attribution to Category 1 predators (such as *Tyto alba*) as the main small-mammal accumulator (López-García et al. 2012a, 2014) in any of the subunits, at least in exclusivity.

Previous studies devoted to small-prey remains from the site also demonstrated a high degree of breakage of leporids in unit III (> 80%) and birds for the full sequence (> 70%). Anatomical profiles of leporids demonstrated proportions closer to accumulations produced by diurnal raptors or mammal carnivores (such as foxes, lynx, or wolves) (Rufà et al. 2014, 2016). However, as well as it is observed in small mammals, the percentages of digested remains (leporids: 9%; birds: 19–35%) and the predominance of light degrees of digestion and in the case of birds also anatomical representation are unlike patterns established for small carnivores and more related to nocturnal raptors. In both cases, a similarity with digestion patterns of *Bubo bubo* was suggested. Anecdotally, one skeletal remain of *Bubo bubo* was recovered in subunit IIa while Strigidae family remains were found in subunits IIIa, IIB, and IIa (Rufà et al. 2016). However, a low percentage of modifications made by carnivores in some avian remains was also observed throughout the

sequence. Small carnivore alternations were also detected in leporid accumulations from unit III (16%), as low percentages of heavy and extreme digestion, which were mainly related to the action of foxes (*Vulpes vulpes*). In the case of small mammals analyzed here, the possible intervention of carnivores through digestion traces has only been detected in subunit IIIb. However, it cannot be rejected that their action incremented breakage rates and biased anatomical profiles in the rest of the sequence.

In summary, these results indicate that the small-mammal assemblages of the Teixoneres Cave were mainly produced by nocturnal raptors and, at least for unit III, most likely by the eagle owl, whose nest or roosting site might have been located near or even inside the cave. This species has been present in the Iberian Peninsula since the Lower Pleistocene and has been the sole species of the genus *Bubo* since the Middle Pleistocene. It is assumed that their past distribution was similar to the present but was probably more southern during stadial periods (Arribas 2004). The eagle owl is a sedentary species that usually nests in cave entrances, cliffs ledges, or rock crevices, using the same place for several years (Mikkola 1983; Andrews 1990; Manzanares 2012; IUCN 2018). It is an opportunistic hunter, including in its diet whatever is available in its hunting territory, which normally extends to around 10 km<sup>2</sup>. It feeds mostly on mammals, but its prey assemblages are highly diverse and reflect the local ecological variability of its nesting area, and include reptiles, amphibians, fish and larger insects. This owl species is the largest in Iberia (2–4 kg) and, thus, tends to include larger preys in its diet, frequently consuming leporids and birds (such as herons and buzzards) (Olsson 1979; Andrews 1990; Manzanares 2012, IUCN 2018). It is a valuable predator for palaeoecological reconstructions, since it generates representative and coherent accumulations



from the ecosystem it exploits (Andrews 1990). In addition, this bird may provide some environmental information due to its common preference by wooded habitats despite being observed in a wide range of environments (Mikkola 1983; IUCN 2018).

### Post-depositional alterations

Post-depositional alterations occurred after small-mammal accumulation but could engender sizable modification in bone conservation and affect skeletal profile quantifications. A common pattern was detected in the post-depositional history of small-mammal remains along the sequence (Table 3; Fig. 2; Appendix 1). Most of the analyzed remains show striations (> 75%), fissures (15–30%), and cracks (2–12%) most likely related to humidity changes. Between 37% (subunit IIIa) and 58% (subunit IIb) of the remains are affected by manganese oxide pigmentation. Another common alteration is chemical corrosion, mainly related to the presence of roots, which affected more of the lower subunits (from 34 to 22%) than the upper ones (around 16%). Occasionally, remains from subunits IIIb and IIIa were covered by isolated cementations (5% and 12%, respectively), being rare in unit II (<2%). Therefore, all features recorded indicated a wet fossiliferous environment where humidity levels underwent some fluctuation, in keeping with cave taphonomic patterns. Finally, few remains in subunits IIIb, IIIa, and IIb were burned and reached carbonization and calcination degrees. The presence of hearths was confirmed at the site, mainly at the entrance of the cave in unit III. In unit II, sediment alterations in form of rubefactions were related to thermal exposure (Rosell et al. 2010a, 2014). Small mammals trapped in the substrate would have been affected by unintentional thermal alterations as a consequence of the surrounding combustion activities (Fernández-Jalvo et al. 2018), suggesting also that a part of the material in direct contact with fire could have disappeared by burning.

The absence of rounding and polish produced by water abrasion supports the idea that small-mammal remains were

not affected by water streams active in the surroundings of the site, supporting previous interpretations based on the absence of round-angle gravel accumulation (Rosell et al. 2010a). Considering the frequency of manganese oxide coating, however, punctual events of flooding cannot be rejected. The taphonomic analysis performed on birds revealed some cases of weathering and trampling (Rufà et al. 2016). In the last case, its apparent absence in small-mammal remains should be clarified in the future with the help of a scanning electron microscope study. The absence of weathering is common in cave deposits where the exposure to light is highly limited. This may confirm the in situ deposition of the small-mammal assemblages and the potentially faster burial of small-mammal remains than that was expected for larger remains considering the low sedimentation rates defined for this cavity (Rosell et al. 2010a, b; Rufà et al. 2016). As was previously observed, the anatomical profiles and breakage rates obtained in each subunit differ from those produced by owls. Post-depositional modifications should be considered as a possible cause of these fractures. Considering the absence of trampling and weathering among small mammals and a low incidence of this damage in medium-size vertebrates (Rufà et al. 2014, 2016), it is complex to consider these agents as the main cause of higher fragmentation rates. Sediment compactions could also play a role in this sense.

### Oxygen isotope compositions of rodent remains

The oxygen isotope composition of the rodent incisor enamel from the Teixoneres sequence ranges from 15.5 to 21.3‰, representing a variation range of 5.8‰ (SD = 1.3) (Fig. 4; Table 1; Table 4). Both mean and median  $\delta^{18}\text{O}_p$  values show little variation among different subunits, ranging from 17.7‰ (subunit IIIa) to 18.5‰ (subunit IIb) and from 17.9‰ (subunit IIIa) to 18.5‰ (subunit IIa), respectively. Differences in mean and median  $\delta^{18}\text{O}_p$  values are around 0.1–0.3‰, showing a homogenous distribution of data inside each subunit. The oxygen isotope compositions of remains from the subfamilies Glirinae and Arvicolinae

**Fig. 4** Oxygen isotope composition (‰ V-SMOW) of rodent incisor enamel from the Teixoneres samples. Box plots and distribution of  $\delta^{18}\text{O}$  values per subunit, with mean (green line) and median (red dashed line) curves. Box plots' bars cover the full extension of the values; boxes extend from the 1<sup>st</sup> to 3<sup>rd</sup> quartiles. Black points, *Apodemus sylvaticus*; blue points, Arvicolinae; yellow points, *Eliomys quercinus*

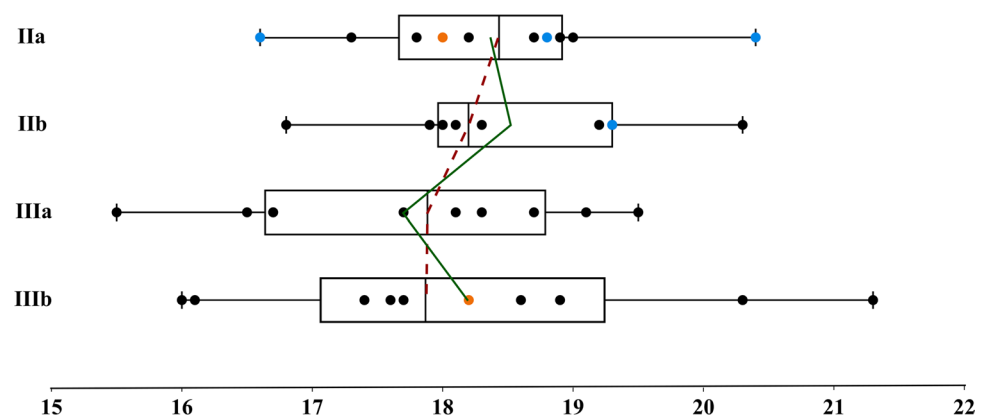


**Table 4** Minimum, maximum, mean, median, standard deviation, and range of oxygen isotope composition of incisor enamel phosphate ( $\delta^{18}\text{O}_p$ ; ‰ V-SMOW) from fossil rodents recovered from Teixoneres Cave samples; conversion to the oxygen isotope composition of meteoric waters ( $\delta^{18}\text{O}_{mw}$ ; ‰ V-SMOW), including minimum, maximum, mean, median, and range; mean annual temperature estimations (MAT; °C), including seasonality and sea level corrections of  $\delta^{18}\text{O}_{mw}$ . SD standard deviation. Present-day samples from Moia are also incorporated to calculate their average temperature, without applying corrections

		IIa	IIb	IIIa	IIIb	Pellet
$\delta^{18}\text{O}_p$	<i>n</i>	10	10	10	10	3
	Min	16.6	16.8	15.5	16.0	19.0
	Max	20.4	20.3	19.5	21.3	19.5
	Mean	18.4	18.5	17.7	18.2	19.1
	Median	18.5	18.2	17.9	18.0	19.2
	Range	3.8	3.5	4.0	5.2	0.5
$\delta^{18}\text{O}_{mw}$	SD	1.0	1.0	1.3	1.7	0.3
	Min	-6.7	-6.6	-7.7	-7.2	-4.8
	Max	-3.6	-3.7	-4.3	-2.9	-4.3
	Mean	-5.3	-5.2	-5.9	-5.4	-4.7
	Median	-5.2	-5.4	-5.7	-5.6	-4.6
	Range	3.2	2.9	3.3	4.3	0.4
MAT	$\delta^{18}\text{O}_{mw}$ (seasonality correction)	-6.3	-6.5	-6.7	-6.7	x
	$\delta^{18}\text{O}_{mw}$ (sea level correction)	-6.9	-7.1	-7.3	-7.3	x
	MAT (°C)	11.8	11.3	10.7	10.8	17.3
	SD	1.3	1.3	1.3	1.3	2.3
	Error margin	2.6	2.6	2.6	2.6	4.5

included in subunits IIa and IIb are consistent with the general  $\delta^{18}\text{O}_p$  range obtained from Murinae remains in the site and have no influence either on the mean or median values. However, in subunit IIa, two of the three values related to Arvicolinae correspond to extreme  $\delta^{18}\text{O}_p$  values increasing the intra-level range. If these samples are not considered, no differences are noticed in average measurements, but the amplitude of this subunit is largely reduced (1.7; SD = 0.6). All sedimentary layers show a normal distribution of data (Shapiro–Wilk's test,  $p$ -value > 0.01).

If the  $\delta^{18}\text{O}_{mw}$  values were estimated from the  $\delta^{18}\text{O}_p$ , the amplitudes recorded inside each subunit of Teixoneres Cave would be lower than the current seasonal amplitude of  $\delta^{18}\text{O}_{mw}$  values recorded at Moia (8.3‰; OIPC data; Bowen 2017) (Fig. 1C; Table 4) and the average seasonal amplitude of  $\delta^{18}\text{O}_{mw}$  values for Iberia (8‰; OIPC data; Bowen 2017; Fernández-García et al. 2019). Tentatively, it can be suggested that analyzed rodent remains most likely accumulated during a preferential period of the year. Indeed, there is a higher probability of accumulating prey by owls during the warm season in Iberia (Chaline 1974; Salamolard et al. 2000; Norrdahl and Korpima 2002; Manzanares 2012; Lagos 2019), as it is indicated by the higher number of murid specimens and the observed oxygen isotope composition of contemporaneous Iberian rodent tooth samples (see discussion in Fernández-García et al. 2019; Royer et al. 2013a, b). Mean and median  $\delta^{18}\text{O}_{mw}$  fossil values are notably higher (from -5.2 to -5.9‰) than the current mean annual  $\delta^{18}\text{O}_{mw}$  values documented at Moia (-7.3‰; Bowen 2017), reinforcing this hypothesis. The minimum value from the sequence, in subunit IIIa, expressed in  $\delta^{18}\text{O}_{mw}$  equivalent to -7.7‰ (Table 2), is not reaching the present-day winter

$\delta^{18}\text{O}_{mw}$  (from -8.8 to -10.5‰; Bowen 2017; Fig. 1B). In contrast, the maximum  $\delta^{18}\text{O}_p$  value record in the subunit IIIb ( $\delta^{18}\text{O}_p = 21.3$ ‰;  $\delta^{18}\text{O}_{mw} = -2.9$ ‰) corresponds to present-day summer oxygen compositions (from -2.6 to -3.8‰; Bowen 2017; Fig. 1B).  $\delta^{18}\text{O}$  values in all subunits do not indicate predation during the cold season but rather coincide with lower mean-medias and higher ranges-SDs in unit III. These results could be either a consequence of climatic instability (if rodent remains are produced in the same period), stadial-interstadial mixings of remains (if mixed faunal communities occurred), and/or changes in seasonality patterns or in the altitude of hunting of the predator. However, it should be considered that the comparison between estimated and modern  $\delta^{18}\text{O}_{mw}$  values is highly speculative considering that several actualistic assumptions should be accepted, including similar humid air masses circulation and similar correspondence between oxygen isotopic values and seasonality patterns.

The eagle owl (*B. bubo*) has been identified in this work as the main cause of small-mammal accumulation in the Teixoneres sequence at least in unit III, in keeping with results obtained for birds and leporids (Rufà et al. 2014, 2016). Today, its breeding operates between January and March in the Iberian Peninsula, incubation lasts about 5 weeks, and the offspring can fly about 2 months after (Manzanares 2012). Consequently, a preferential accumulation is proceed during spring and beginning of summer, knowing that its foraging is usually increment coinciding with their breeding period (Salamolard et al. 2000; Norrdahl and Korpima 2002; Manzanares 2012; Lagos 2019). Taphonomic studies on avian remains, which probably share their origin with small mammals, could help to infer the

seasonality of human and carnivore/raptor occupations. Few medullary bones among avian remains (*Pica pica* in level IIa and *Pyrrhocorax* spp. in level IIIb) have been observed, tentatively suggesting that at least part of the bird assemblage was accumulated during spring (Rufà et al. 2016).

Moreover, zooarchaeological and taphonomic analyses reflect the presence of carnivores (mainly cave bear and hyena) alternated with Neanderthal occupations, and the evidence associated with humans and carnivores does not usually overlap temporally (Rosell et al. 2010a, b, 2017). Regarding carnivores, bears are known to use the cave mainly for hibernation during winter months, but patterns of hyenas and small carnivores are unknown (Rosell et al., 2017). From a combination of tooth microwear, cementum analysis, and dental eruption patterns in cervids and equids from the site, Sánchez-Hernández et al. (2014, 2016, 2020b) suggested that there were repeated short-term hominin occupations at the site within the same season of the year, probably in summer for subunit IIa; in autumn and early winter for subunit IIb; summer and winter, in subunit IIIb; and repeated and short occupations in all seasons for subunit IIIa. Equids, however, were mainly hunted during late spring and summer. These periods of frequentation of the cave may be related to an abundance of cervids and equids in the territory (Sánchez-Hernández et al. 2014, 2016; Rosell et al. 2017; Picin et al. 2020). Based on these interpretations of short-term human occupations and the preferential use of the cave by owls in spring, in addition to noted carnivore dynamics, in general, no coexistence between humans and owls and/or carnivores can be supported. This reinforces the absence of temporal contact between them underlined by previous taphonomic and zooarchaeological studies, which demonstrate long periods without human occupation of the

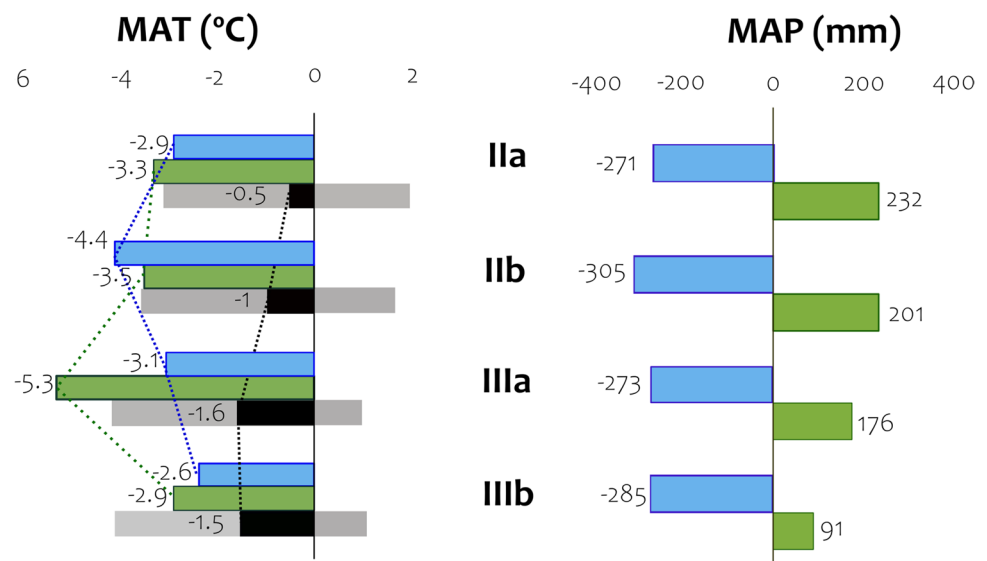
site (Rosell et al. 2010a, b, 2017; Rufà et al. 2014, 2016; Sánchez-Hernández et al. 2014).

## Reconstruction of past temperatures

Mean annual temperature (MAT) was calculated based on the median  $\delta^{18}\text{O}_p$  of each sedimentary subunit (Fig. 5). The estimated MATs vary between  $10.7 \pm 2.6$  °C (subunit IIIa) and  $11.8 \pm 2.6$  °C (subunit IIa). These temperatures are lower than the current MAT recorded at Moià ( $12.3$  °C; Climate-Data.org; Fig. 1B), with differences ranging from  $-0.5$  to  $-1.6$  °C. Along the sequence, MAT differences are small ( $\leq 1.1$  °C). Therefore, based on oxygen isotope compositions, a homogenous and milder climate without notable changes is indicated; however, a slight increase in temperatures from lower subunits ( $10.8$ – $10.7$  °C) to upper ones ( $11.3$ – $11.8$  °C) has been detected.

Additionally, oxygen isotope compositions of the remains recovered in the modern pellet from the Moià region provide homogenous values of  $19.1 \pm 0.3\text{‰}$  ( $-4.6 \pm 0.4\text{‰}$  in  $\delta^{18}\text{O}_{mw}$ ), which is especially relevant considering those remains belong to two different species (Table 4). Considering  $\delta^{18}\text{O}_{mw}$  at the place of sample recovery (at 1000 m a.s.l.; OIPC data; Bowen 2017), the pellet records could be coincident with May–June ( $-5.4/ -4.2\text{‰}$ ) or with September ( $-4.5\text{‰}$ ). The pellet was recovered in August in a semi-dry state. Thus, the most plausible explanation is that this pellet recorded information from May to July, considering that *Apodemus* and *Microtus* incisors reflected the one or two last months of life of the animal (Klevezal et al. 1990; Klevezal 2010; Royer et al. 2013a; Fernández-García et al. 2019). The mean  $\delta^{18}\text{O}_{mw}$  value of the pellet equals an average temperature of  $17.3$  °C, close to the current mean temperature recorded for June (Climate-Data.org). This mean

**Fig. 5** Mean annual temperature (MAT) and mean annual precipitation (MAP) estimations for the Teixoneres Cave sequence with respect to present-day climate in Moià (MAT =  $12.3$  °C; MAP =  $749$  mm; Climate-data.org), considering the bioclimatic model (in blue) and mutual ecogeographical range (in green) methods, and the oxygen isotope compositions (in black) of rodent phosphates samples (error is presented in grey fringe)



temperature is notably higher than that for the fossil samples of the Teixoneres Cave but is generally consistent with temperature and  $\delta^{18}\text{O}_{\text{mw}}$  annual variations for the region, validating established correlations in that region. The incisor recovered from an unknown accumulation of disintegrated pellets recorded 16.1‰ and does not correspond to the same season of accumulation, reporting lower  $\delta^{18}\text{O}_{\text{mw}}$  values (−7.2‰), probably out of the warm season.

The MATs calculated from the  $\delta^{18}\text{O}_{\text{p}}$  of Teixoneres samples are compared with two other methods of palaeoclimatic reconstruction usually used for small-mammal assemblages: the bioclimatic model (BM) and the mutual ecogeographic range (MER) (Fig. 5; Appendixes 3 and 4). Both methods provide lower temperatures than present day: the BM method from −2.6 to −4.4 °C, whereas MER estimations from −3.3 to −5.3 °C.  $\delta^{18}\text{O}$  air temperature estimations offer the highest temperatures, recording similar trends as MER temperature reconstructions, but with notably higher estimations than this method (+1.4/+3.7 °C with respect to MER). Thus, all the three methods show highly in agreement trends and confirm lower MATs than present day in Moià, a pattern enforced when mean oxygen isotope values are considered (Table 4). In general, homogenous temperature patterns are observed along the sequence with independence of the method considered, although some discrepancies can be observed in subunit IIIa. Despite these differences, BM and MER method estimations generally fall within the confidence interval of  $\delta^{18}\text{O}$  estimations and inter-level differences considering equivalent methods are small. Whereas the MER method records mean annual precipitations (MAP) higher than present day in Moià (+44/+682 mm), the BM method supports the opposite trend, with all levels lower than nowadays (−271 to −305 mm). However, both methods underline slight pluviometry changes along the sequence, with homogenous climatic conditions again.

Discrepancies between these methods can be explained by several factors. BM and MER are both qualitative methods, just transforming species composition changes and the into quantifiable climatic terms. This operation is mainly based on the modern biogeographic distribution of species and linking them to specific biomes or climatic parameters, respectively. The geographical scale considered from both methods either the climatic quantifiable parameters between both methods differed, and this can lead to inconsistencies between methods estimations. BM is based on biome classification (and their derived climatic information) from species spread through Eurasian, whereas MER considers species distribution on Iberia, which directly links to regional temperatures and precipitations. Moreover, small-mammal geographical distribution can be related to climatic factors but also can be a consequence of other causes, such as anthropic pressure, human modification on the ecosystems, species competition, predation, or just the existence

of non-analogue faunal associations in the past (Blain et al. 2016; Lyman 2017; Royer et al. 2020). Otherwise, stable isotope estimations are expected to be less susceptible to archaeological biases, but the sampling method and actualistic assumptions linked to the empirical correlations as well as correlation selection according to the taxonomic group and geographical scale of the dataset considered may conditionate the final temperature estimation (detailed discussion on Fernández-García et al., 2019; 2020). This means that the comparison between palaeoclimatic reconstruction methods, as well as the comparison with other environmental proxies of a site, is key to reach a reliable interpretation.

### Teixoneres sequence and Neanderthal ecological context

Short-term Neanderthal occupations occurred in 2, in alternation with mammalian carnivore and raptor activities in the site. Competition and cohabitation theories between carnivores/raptors and humans have been highly discussed (e.g., Rosell et al. 2010a, b, 2017; Picin et al. 2020). It is constantly evaluated inside the Middle Palaeolithic, how climatic conditions should play a decisive role in the subsistence strategies and mobility patterns of these human populations and their migration routes or if in some degree this strengthens their adaptative behaviour. The calibrated radiocarbon dates for the Teixoneres Cave sequence (Talamo et al. 2016) allow us to approach global climatic data and the contemporaneous deposition of these units and evaluated how and which of these climatic fluctuations have been recorded at the local scale. MIS 3 (ca. 60–30 ka) is a period characterized by a continuous oscillation of climatic events, including strong and brief cold episodes, such as stadials and Heinrich Events (e.g., Fletcher and Sánchez-Goñi 2008; Fletcher et al. 2010b; Wolff et al. 2010; Rasmussen et al. 2014). However, the southern Europe peninsulas, and particularly the Mediterranean basin, are usually less prone to major climate changes resulting in significant remobilizations of animal communities.

This research has shown that climatic conditions in the Teixoneres Cave surroundings were generally homogenous and always cooler and wetter than nowadays, but slight differences found between lower subunits (unit III) and upper subunits (unit II) from the analysis of small vertebrates of Teixoneres Cave should be addressed. Small variations in the fauna spectrum, in terms of presence/absence and abundances, suggest slight environmental changes notably between subunits (López-García et al. 2012a). For instance, the presence of the Mediterranean species, *Microtus (T.) duodecimcostatus*, is higher (12–14%) in unit III and lower in subunit IIb (<3%), disappearing next in upper subunit IIa. The relative abundance of *A. sylvaticus*, a generalist species with a preference for woodland environments, is remarkably high for subunit IIIb (41%) (Appendix 2). The progressive



decrease in woodland-dwelling (*A. sylvaticus*, *E. quercinus*, and *G. glis*) and Mediterranean species (mainly *M. (T.) duodecimcostatus*) in favor of open-environment species with mid-European requirements (*M. arvalis* and *M. agrestis*) between units III and II suggests a woody environment for level III changing to more open landscape in level II. In subunit IIIa, some cold-dependent species also appear among small mammals such as *Chionomys nivalis* and *M. (T.) gerbei* and are noticed equally in subunit IIb (*C. nivalis*, *Neomys fodiens*, and *S. coronatus*) (Appendix 2), which suggest a cooling phase. Nonetheless, relative species abundances of small mammals are also not fully in agreement with the pattern observed in northeastern Iberia faunal assemblages for very cold and moist conditions (López-García et al. 2014; Fernández-García et al. 2016).

According to the oxygen isotope analysis (Table 5), subunits IIb and IIIa have higher dispersion of  $\delta^{18}\text{O}$  values (4–5.2‰) and lower  $\delta^{18}\text{O}$  averages mean values, tentatively related to cooler conditions than in upper subunits, or at least to punctuated climatic instability. Based on the geochemical record, MATs estimated are the lowest of the sequence (IIb:  $10.8 \pm 2.6$  °C; IIIa:  $10.7 \pm 2.6$  °C). Moreover, unit III contents reflect drier conditions than for unit II when calculated by the MER method, while the BM method provided notably lower precipitation rates for all four subunits. Contrary to unit III, rodent teeth oxygen isotope compositions of the upper subunits (IIb–IIa) have higher  $\delta^{18}\text{O}$  means and medians (18.2–18.5‰), a lower intra-level amplitude (3.5–3.8‰), and lower standard deviations (1–1.1‰) (Table 5). According to  $\delta^{18}\text{O}$  estimations, MATs are slightly higher than for unit III (IIb =  $11.3 \pm 2.6$  °C; IIa =  $11.8 \pm 2.6$  °C), but differences between both units are tiny (+0.5/ +1 °C), with both units characterized by cooler conditions than current climatic records. In this case, the BM method coincides in inferring for subunit IIb the coldest (–4.4 °C) and driest (–305 mm) conditions than present day in the region, but not for the MER method. Thus, some discrepancies are found between methods and with previous environmental studies, particularly for unit III which was correlated with an interstadial period and indicated that conditions were relatively temperate and humid (López-García et al. 2012a). Owls are confirmed as the primary agent responsible for most small-mammal inputs, so taphonomic causes are primarily rejected as the main explanation for these inconsistencies, considering the opportunist behaviour of the main accumulator, the eagle owl.

In comparison, large-mammal assemblages of this unit reflect a faunal mixture in which temperate ungulate species are predominant and cold-adapted taxa are very scarce. Occurrences of *Mammuthus primigenius* have been noted in unit III, whereas *Coelodonta antiquitatis* remains have been identified in units III and II (Álvarez-Lao et al. 2017), which are interpreted as indicators of cold and dry pulsations. This

pattern of cold and temperate faunal mixture is relatively common in other Iberian assemblages with the presence of this species, suggesting that cold-adapted taxa only reached the Peninsula occasionally and during the coldest episodes of the Pleistocene. Sporadic presence of cold-adapted fauna is also observed in level J (ca.44 ka BP) from Arbrede cave (Ruff et al. 2018; Sánchez-Hernández et al. 2020b) and is widely documented into contemporaneous sites from the Cantabrian area (Álvarez-Lao et al. 2015; Álvarez-Lao and Méndez 2016; Rodríguez-Almagro et al. 2021). Colder and dryer pulsations were suggested for subunit IIIa from use-wear analysis on ungulate teeth, which reveals punctuated increase of grazer behaviour for cervids and equids (Sánchez-Hernández et al. 2020a, b).

The complex formation of horizontal subunits IIb and IIIa should be considered. It is interpreted as a palimpsest between recurrent short-term human occupations in the entrance of the cave with mixed contributions by predators inhabiting the inner part of the cave during different periods (Rosell et al. 2010a, b, 2017; Sánchez-Hernández et al. 2014; Talamo et al. 2016; Picin et al. 2020). A complete spatial analysis of Unit III has confirmed the important nature of this palimpsest attesting frequent and repeated human occupations in a consistent and similar way for more than 7000 years (Zilio et al. 2021). In climatic terms, we proposed as the most plausible explanation that these subunits are the result of slow sedimentation rates that promoted the overlap between different climatic events, precluding the isolation of different stadial and interstadial events from the faunal spectra. A mix of species dependent on either temperate or cold conditions points to the sedimentary recording of punctual cold events in agreement with the occurrence of the woolly mammoth and the woolly rhinoceros, but that under current small-mammal analysis is not possible to isolate, giving a general faunal spectrum that seems globally temperate. Probably, small mammals from unit III are recording a long-term environmental trend based on temperate conditions and woody landscape, which is coincident with the palynological sequence (Ochando et al. 2020).

Similarly, the cooler and drier conditions detected by small-mammal assemblages in unit II were tentatively associated with cold events and even to Heinrich Event peaks of MIS 3 (López-García et al. 2012a, 2014), which could be consistent with the punctual occurrence of *C. antiquitatis* in this level (Álvarez-Lao et al. 2017). But considering the new radiometric dates of this unit (ca. 33–44 ka) (Talamo et al. 2016), it should correspond to HE4 if this correlation is accepted (Hemming 2004). However, this climatic correlation with an exceptional cold and dry event cannot be fully supported by the results of this work. Moreover, small mammals are not directly linked to human presence in the cave and their accumulation is produced in other seasons than human visits to the cave. This is a complex issue to

**Table 5** Previous palaeoenvironmental approaches to Teixoneres sequence and results from this work. Mean annual temperature and mean annual precipitation estimations are included, according to the bioclimatic model (BM) method, mutual ecogeographic range (MER) method, and oxygen isotope compositions ( $\delta^{18}\text{O}$ )

Unit	Subunits	Pollen and Charcoals (López-García et al., 2012a, b)	New data pollen (Ochando et al., 2020)	Large mammals and palaeodiet (Álvarez-Lao et al., 2017; Carlos-Sánchez et al., 2020a, 2020b)	Small vertebrates (López-García et al., 2012a, b)	Oxygen isotope analysis (This work)	Small mammals' predator (This work)	Past temperatures (this work & López-García et al., 2012a, b)	Past precipitations (this work & López-García et al., 2012a, b)
II (ca. 33–44 ka)	IIa	Open woodland and meadows. Dry conditions in relation to steppe taxon <i>Artemisia</i> (IIa). <i>Pinus</i> , <i>Quercus</i> and angiosperm charcoals	Mix oak-pine forest. AP > 65% with evergreen <i>Quercus</i> (16–47%), <i>Pinus nigra-sylvestris</i> (8–17%), and <i>Juniperus</i> (1–17%). Herbs: Poaceae, <i>Artemisia</i> are dominant in NAP	Abundant temperate-adapted species (mainly <i>Cervus elaphus</i> followed by equids), presence of <i>Coelodonta antiquitatis</i> , and higher presence of <i>Rupicapra</i> and <i>Capra pyrenaica</i> and <i>Sus scrofa</i> . Open forest and rocky landscape	Abundant European species ( <i>M. agrestis</i> , <i>M. arvalis</i> ), scarce presence of forest dwellers ( <i>A. sylvaticus</i> ), and absence of Mediterranean species. Cooler and drier phase related to stadial. Open woodland	Homogenous, low amplitude, and the highest median. Stable period	Nocturnal raptors; digestion = 43%	BM = 9.4 °C/ MER = 9 °C/ $\delta^{18}\text{O}$ = 11.8 ‰	BM = 477 mm/ MER = 981 mm
	IIb	Mix oak-pine forest. AP = 58–74%, dominated by evergreen <i>Quercus</i> (17–52%), <i>Juniperus</i> (2–13%), <i>Pinus</i> (9–20%). Herbs: Poaceae, <i>Artemisia</i> , Amaranthaceae	Mix oak-pine forest. AP = 58–74%, dominated by evergreen <i>Quercus</i> (17–52%), <i>Juniperus</i> (2–13%), <i>Pinus</i> (9–20%). Herbs: Poaceae, <i>Artemisia</i> , Amaranthaceae	Abundant European species ( <i>M. arvalis</i> , <i>M. agrestis</i> , <i>M. (T.) gerbei</i> , <i>C. nivalis</i> ), scarce presence of forest dwellers ( <i>A. sylvaticus</i> ), and scarce Mediterranean species ( <i>M. (T.) dioecimcostatus</i> ). Cooler and drier phase related to stadial. Open woodland, increase in dry meadows and rocky areas	Abundant European species ( <i>M. arvalis</i> , <i>M. agrestis</i> , <i>M. (T.) gerbei</i> , <i>C. nivalis</i> ), scarce presence of forest dwellers ( <i>A. sylvaticus</i> ), and scarce Mediterranean species ( <i>M. (T.) dioecimcostatus</i> ). Cooler and drier phase related to stadial. Open woodland, increase in dry meadows and rocky areas	Homogenous, the lowest amplitude, and high median. Stable period	Nocturnal raptors; digestion = 31%	BM = 7.9 °C/ MER = 8.8 °C/ $\delta^{18}\text{O}$ = 11.3 ‰	BM = 444 mm/ MER = 950 mm

Table 5 (continued)

Unit	Subunits	Pollen and Charcoals (López-García et al., 2012a, b)	New data pollen (Ochando et al., 2020)	Large mammals and palaeodiet (Álvarez-Lao et al., 2017; Carrión-Sánchez et al., 2020a, 2020b)	Small vertebrates (López-García et al., 2012a, b)	Oxygen isotope analysis (This work)	Small mammals' predator (This work)	Past temperatures (this work & López-García et al., 2012a, b)	Past precipitations (this work & López-García et al., 2012a, b)
III (ca. 44–51 ka)	IIIa		Mix oak-pine forest. AP > 87%. Evergreen <i>Quercus</i> is outstanding (7–56%); <i>Pinus halepensis-pinea</i> (2–31%), <i>Juniperus</i> (1–30%), and <i>Pinus nigra-sylvestris</i> (14–16%). Several fungal spore	Abundant temperate-adapted (mainly <i>Cervus elaphus</i> and some equids) but scarce cold-adapted species ( <i>Mammuthus primigenius</i> in IIIa and <i>Coelodonta antiquitatis</i> in IIIb). Open forested landscape with patchy areas. Increase of wild ass browser behaviour indicates wetter conditions in IIIb, whereas increasing in grass consumption by equids and cervids indicates open areas and worsening conditions for IIIa	Mediterranean species ( <i>M. (T.) duodecimcostatus</i> , <i>I. cabreriae</i> ), Mid-European species ( <i>M. arvalis</i> , <i>M. agrestis</i> , <i>C. nivalis</i> , <i>M. (T.) gerbet</i> ), and forest dwellers ( <i>A. sylvaticus</i> ). Temperate and humid phase related to interstadial. Open woodland but increase in humid meadows and water	Heterogenous, medium amplitude, the lowest median. Unstable	<i>Bubo bubo</i> ; digestion = 36%	BM = 9.2 °C/ MER = 7 °C/ $\delta^{18}O = 10.7$ °C	BM = 476 mm/ MER = 925 mm
	IIIb		Mix oak-pine forest. AP = 60%; <i>Pinus</i> (11–26%); <i>Quercus</i> (14–46%); <i>Juniperus</i> (3–8%), <i>Casanea</i> , <i>Betula</i> , <i>Corylus</i> . Herbs: Poaceae, <i>Artemisia</i> , Amaranthaceae		Abundant presence of forest dwellers ( <i>A. sylvaticus</i> ), presence of Mediterranean ( <i>M. (T.) duodecimcostatus</i> ), and Mid-European ( <i>M. arvalis</i> , <i>M. agrestis</i> ) species. Temperate and humid phase related to interstadial. Open woodland	Heterogenous, low median, and the largest amplitude. Unstable	<i>Bubo bubo</i> + carnivores occasional inputs; digestion = 36%	BM = 13.4 °C/ MER = 9.7 °C/ $\delta^{18}O = 10.8$ °C	BM = 463 mm/ MER = 840 mm

be addressed for climatic interpretation because it cannot be evaluated if it is just in different seasons from not very distant years. Considering that there is not a clear spatial or stratigraphical distinction between small mammals and archaeological remains in the cave sediments, we assumed that small mammals and remains derived from human occupations even if being introduced in different seasons or seasons from different years are coincident in few-millennial sedimental accumulation. Thus, if abrupt climatic changes are experienced could be detected from both approaches. Nevertheless, only a complete spatial distribution study and direct radiocarbon dating on small mammals remains, as well as a comparison with biochemical analyses on hunted ungulates, could give us some clues on the overlapping and the chronological resolution.

The present study underscores that despite these punctual cold episodes marked by the presence of small- and large-mammal cold-adapted species, the local-to-regional ecological conditions experienced by Neanderthal groups in this region were milder and highly conservative; differences of less than 1 °C between all subunits are estimated considering oxygen isotope compositions of rodent teeth and with mean standard deviations < 1 °C for MER and BM methods. Recent works point to the Late Pleistocene “tundra-steppe” biome extension to southern latitudes as one of the main drivers in *C. antiquitatis* spread waves (Puzachenko et al. 2021; Rodríguez-Almagro et al. 2021). However, palynological studies of the Teixoneres Cave sequence (Ochando et al. 2020) confirmed that the global trend is a dense oak-pine forest in all subunits, with arboreal pollen oscillating between 60 and 90% during the whole sequence and with unfrequented high values of oak pollen, considering that pine forests usually dominated in the Mediterranean area (Allué et al. 2017; Carrión et al. 2018; Ochando et al. 2020, 2021). Cold component pollen taxa (such *Artemisia*, *Poaceae*, *Amaranthaceae*, *Erica*, *Ephedra fragilis*) experienced punctuated increases from subunits IIb and IIIb but are anecdotal. Indeed, the woodland component is always the dominant type of landscape considering small vertebrates in spite of faunal frequencies (López-García et al. 2012a).

These results are in agreement with regional interpretations of MIS 3 equivalent small-mammal studies performed in Abric Romaní rock-shelter (Burjachs et al. 2012; Fernández-García et al. 2018, 2020) and Xaragalls cave (López-García et al. 2012a; Fernández-García et al. 2019). In both sequences, a detailed climatic characterization based on small-mammal assemblages has been accomplished through a combination of taxonomy, taphonomy, and oxygen isotope studies. Oxygen isotope compositions of rodent bioapatite phosphate are usually homogenous with higher and less scattered values than equivalent studies from northern latitudes (Royer et al. 2013a, b, 2014). Environmental reconstruction

proposed for these sites points always to wetter, cooler, and homogenous climatic cycles, and forested areas next to the settlements. A general trend is observed from northeastern Iberia small-mammal communities (López-García et al. 2014; Fernández-García et al. 2016), but also extent to the Mediterranean area, as documented in Arbreda Cave (López-García et al. 2015), Terrasses de la Riera dels Canyars (López-García et al. 2013), Cova del Gegant (López-García et al. 2012b), Cova del Coll Verdaguer (Daura et al. 2017), El Salt (Fagoaga et al. 2018, 2019), or Gorham’s Cave (López-García et al. 2011). Pollen and charcoal analyses conducted in some of these sites agree on a predominance of forests composed of conifers (mainly *Pinus* and *Juniperus*) and evergreen and deciduous species (González-Sampérez et al. 2010; Burjachs et al. 2012; Carrión 2012; Allué et al. 2017; Daura et al. 2017). Stable climatic conditions, which prevailed during MIS3, sheltered a high biodiversity during the Late Pleistocene as also proposed for the Levantine area (including the MIS3 records from Cova de les Malladetes and Cova de les Cendres) based on charcoal, pollen, and faunal studies (Real et al. 2021).

These findings are in line with research undergone on large-mammal faunas palaeodiet traces. Sánchez-Hernández et al. (2020a) reconstruct the Neanderthal settlement patterns for several archaeological sites in the Mediterranean area (Arbreda, Teixoneres, Abric Romaní, and El Salt), based on tooth wear and cementum analysis. From this research can be indirectly inferred patched areas with comparable proportions of open and wooded areas. Environmental oscillations are buffered for these sites that are continuously visited by human groups and are not expected to alter logistic models of settlement and mobility of Neanderthal groups, based on short-seasonal movements. Moreover, from the comparison on feeding behaviours of ungulates (*Cervus elaphus*, *Equus ferus*, and *Equus hydruntinus*) from Teixoneres and Arbreda caves, Sánchez-Hernández et al. (2020b) observed a maintenance of the same dietary behaviour of red deer and horses in both sites pointing to steady local environmental conditions over a long-term scale, independently of altitude. The dietary features observed for ungulates correlate well with the relative temperate and humidity conditions for the studied assemblage and from regional small-mammal trends already mentioned.

Among the less abrupt climatic conditions widely explained that Iberia experienced during the Last Glacial, Teixoneres Cave as well as other archaeological sites of northeastern Iberia underline how the Mediterranean corridor allows optimal conditions for the maintenance of Neanderthal populations. The high environmental and climatic variability offered by the Iberian Peninsula not only by its southern position but also by the high variability of micro-environments provides the recurrent mosaic landscape that oscillated from more open to close forests (Allué et al. 2017;



Fernández-García et al. 2020; Ochando et al. 2021; Real et al. 2021). These Neanderthal populations take advantage of the temperate forest provided by the Mediterranean area. This allows long-term preservation of a high diversity of resources available to be exploited by Neanderthal groups, which even when fluctuating in location or abundance probably did not pose a problem for Neanderthal subsistence considering their behavioural plasticity. It does not exclude, however, that punctual colder pulsations were experienced and affected past ecosystems, as cold-adapted large and small faunal episodes have revealed. But, probably, the mosaic landscapes sustained in the Mediterranean area allowed maintenance of these human group subsistence strategies, as well as their preys and their usual plant resources.

## Conclusions

The analyzed small mammals accumulated in the cave mainly due to predation by nocturnal raptors. In agreement with taphonomic analyses performed on bird and leporid remains, the main agent corresponds to the eagle owl (*Bubo bubo*), at least in unit III. *Bubo bubo*-type predators probably maintained their roosting or nesting place in the Teixoneres Cave during the formation of unit II, but other owls may have contributed with small-mammal inputs as well. Consistent with other small-prey studies in the sequence, the punctual intervention of mammal carnivores can be suggested for level IIIb. Among post-depositional agents, plant activity, cracking, and manganese oxide coating are common, indicating a wet fossiliferous microenvironment with humidity fluctuations, where abundant breakage rates are observed. Some burned remains have been detected in relation to unintentional burning.

The medium to low intra-level ranges of oxygen isotope values point to a preferential accumulation of rodents, probably during the spring season. This period of frequentation by owls is in accordance with previous seasonality inferences based on several medullary bones of birds, which share a common origin with small mammals, and results generally differed from use-wear and dental eruption analyses on ungulates, mainly related to hominin contributions to the cave. According to  $\delta^{18}\text{O}$  estimations of temperatures, slightly cooler climatic conditions than present were recorded ( $-1.6/-0.5\text{ }^{\circ}\text{C}$ ). The observed trend is globally in agreement with MER estimations, which recorded colder MATs ( $-2.9/-5.3\text{ }^{\circ}\text{C}$ ), but differ in unit III with BM, which recorded MATs similar to present-day levels ( $+0.1/+1.1\text{ }^{\circ}\text{C}$ ). Both methods calculated wetter conditions than during present day ( $+44\text{ mm}/+682\text{ mm}$ ).

Only slight changes are observed between lower unit III and unit II, which may tentatively be related to some climatic

instability. This trend is not fully in agreement with previous environmental interpretations based on small-mammal relative abundances but may be in keeping with the occasional occurrence of cold-dependent large and small-mammal species. These inconsistencies between methods could point to a palimpsest where stadial and interstadial events overlapped, especially in subunit IIIa. However, oxygen isotope compositions of analyzed rodent teeth underscore the presence of rather stable climatic conditions across the sequence, with little variation between subunits, including those expressed in MAT ( $<1\text{ }^{\circ}\text{C}$ ). A favorable and milder climatic scenario is confirmed for the Mediterranean area in combination with constant presence of open forests that potentially sustained the faunal and vegetal resources preferred by Neanderthal groups.

**Supplementary Information** The online version contains supplementary material available at <https://doi.org/10.1007/s12520-022-01564-9>.

**Acknowledgements** We want to express our sincerest gratitude to all researchers and fieldwork team of the Coves del Toll project, which made possible during repeated field campaigns the recovery of small-mammal remains used in this work. The research in Teixoneres is supported by projects SGR 2017-836 and CLT009/18/00055 from the Generalitat de Catalunya. M. F. G., F. R., R. B., A. R., and J. R. research is supported by the Spanish Ministry of Science and Innovation through the projects PID2019-103987GB-C31, PGC2018-093925-B-C32, PID2019-104949GB-I00, and PID2020-114462GB-I00, and the “María de Maeztu” excellence accreditation (CEX2019-000945-M). We also thank Christiane Denys and Emmanuelle Stoetzel for their help with the taphonomic analysis and the Laboratoire de Géologie of Lyon, especially Jean Goedert and Romain Amiot for their active advice during the isotope analysis. M. Fernández-García was a beneficiary during this manuscript elaboration of a PhD scholarship funded under the Erasmus Mundus Programme – International Doctorate in Quaternary and Prehistory by the European Commission (2015-1611/001-001-EMJD) and currently her research is funded by the European Research Council under the European Union’s Horizon 2020 Research and Innovation Programme (grant agreement No. 818299- SUBSILIENCE project). J. M. López-García and Ruth Blasco are supported by Ramón y Cajal contracts (RYC-2016-19386; RYC2019-026386-I) with financial sponsorship from the Spanish Ministry of Economy and Competitiveness. A. Rufà is currently a beneficiary of the Individual Call to Scientific Employment Stimulus—3rd Edition promoted by the Portuguese FCT (2020.00877.CEECIND).

**Author contribution** Conceptualization, investigation, material preparation, data collection, and formal analysis were mainly performed by M. Fernández-García. J. M. López-García, A. Royer, and C. Lécuyer were actively involved in the conceptualization, formal analysis, investigation, resources, and writing and editing of the original draft. R. Blasco, F. Rivals, J. Rosell, and A. Rufà provide guidance in the conceptualization, resources, and reviewing-editing of the manuscript. The first draft of the manuscript was written by M. Fernández-García, and all authors commented on previous versions of the manuscript. All authors read and approved the final manuscript.

**Funding** Open Access funding provided thanks to the CRUE-CSIC agreement with Springer Nature.

## Declarations

**Conflict of interest** The authors declare no competing interests.

**Open Access** This article is licensed under a Creative Commons Attribution 4.0 International License, which permits use, sharing, adaptation, distribution and reproduction in any medium or format, as long as you give appropriate credit to the original author(s) and the source, provide a link to the Creative Commons licence, and indicate if changes were made. The images or other third party material in this article are included in the article's Creative Commons licence, unless indicated otherwise in a credit line to the material. If material is not included in the article's Creative Commons licence and your intended use is not permitted by statutory regulation or exceeds the permitted use, you will need to obtain permission directly from the copyright holder. To view a copy of this licence, visit <http://creativecommons.org/licenses/by/4.0/>.

## References

- Allué E, Solé A, Burguet-Coca A (2017) Fuel exploitation among Neanderthals based on the anthracological record from Abric Romaní (Capellades, NE Spain). *Quat Int* 431:6–15. <https://doi.org/10.1016/j.quaint.2015.12.046>
- Álvarez-Lao DJ, Méndez M (2016) Latitudinal gradients and indicator species in ungulate paleoassemblages during the MIS 3 in W Europe. *Palaeogeogr Palaeoclimatol Palaeoecol* 449:455–462. <https://doi.org/10.1016/j.palaeo.2016.02.050>
- Álvarez-Lao DJ, Rivals F, Sánchez-Hernández C et al (2017) Ungulates from Teixoneres Cave (Moià, Barcelona, Spain): presence of cold-adapted elements in NE Iberia during the MIS 3. *Palaeogeogr Palaeoclimatol Palaeoecol* 466:287–302. <https://doi.org/10.1016/j.palaeo.2016.11.040>
- Álvarez-Lao DJ, Ruiz-Zapata MB, Gil-García MJ et al (2015) Palaeoenvironmental research at REXIDORA Cave: new evidence of cold and dry conditions in NW Iberia during MIS 3. *Quat Int* 379:35–46. <https://doi.org/10.1016/j.quaint.2015.04.062>
- Andrews P (1990) Owls, Caves and Fossils. Predation, preservation and accumulation of small mammal bones in caves, with an analysis of the Pleistocene Cave Faunas from Westbury-sub-Mendip, Somerset, UK. The University of Chicago, Chicago
- Arribas Ó (2004) Fauna y paisaje de los Pirineos en la Era Glaciar. Lynx, Barcelona
- Bennàsar M (2010) Tafonomía de micromamíferos del Pleistoceno Inferior de la Sierra de Atapuerca (Burgos): Sima del Elefante y Gran Dolina. Universitat Rovira i Virgili (Tarragona)
- Bennàsar M, Cáceres I, Cuenca-Bescós G (2016) Paleoeological and microenvironmental aspects of the first European hominids inferred from the taphonomy of small mammals (Sima del Elefante, Sierra de Atapuerca, Spain). *Comptes Rendus - Palevol* 15:635–646. <https://doi.org/10.1016/j.crpv.2015.07.006>
- Bernard A, Daux V, Lécuyer C et al (2009) Pleistocene seasonal temperature variations recorded in the  $\delta^{18}O$  of *Bison priscus* teeth. *Earth Planet Sci Lett* 283:133–143. <https://doi.org/10.1016/j.epsl.2009.04.005>
- Blain HA, Lozano-Fernández I, Agustí J et al (2016) Refining upon the climatic background of the Early Pleistocene hominid settlement in western Europe: Barranco León and Fuente Nueva-3 (Guadix-Baza Basin, SE Spain). *Quat Sci Rev* 144:132–144. <https://doi.org/10.1016/j.quascirev.2016.05.020>
- Bowen GJ (2017) The Online Isotopes in Precipitation Calculator, Version 3.1 (4/2017). <http://waterisotopes.org>
- Burjachs F, López-García JM, Allué E et al (2012) Palaeoecology of Neanderthals during Dansgaard-Oeschger cycles in northeastern Iberia (Abric Romaní): from regional to global scale. *Quat Int* 247:26–37. <https://doi.org/10.1016/j.quaint.2011.01.035>
- Bustos-Pérez G, Chacón MG, Rivals F et al (2017) Quantitative and qualitative analysis for the study of Middle Paleolithic retouched artifacts: unit III of Teixoneres cave (Barcelona, Spain). *J Archaeol Sci Reports* 12:658–672. <https://doi.org/10.1016/j.jasrep.2017.02.021>
- Carrión JS (2012) Paleoflora y paleovegetación de la Península Ibérica e Islas Baleares: Plioceno-Cuaternario. Ministerio de Economía y Competitividad - Universidad de Murcia, Murcia
- Carrión JS, Ochando J, Fernández S et al (2018) Last Neanderthals in the warmest refugium of Europe: palynological data from Vanguard Cave. *Rev Palaeobot Palynol* 259:63–80. <https://doi.org/10.1016/j.revpalbo.2018.09.007>
- Chaline J (1974) Les proies des rapaces. Doin Éditeurs, Paris
- Climate-Data.org. (2018): <https://es.climate-data.org/>
- Comay O, Dayan T (2018) Taphonomic signatures of owls : new insights into micromammal assemblages. *Palaeogeogr Palaeoclimatol Palaeoecol* 492:81–91. <https://doi.org/10.1016/j.palaeo.2017.12.014>
- Crowson RA, Showers WJ, Wright EK, Hoering TC (1991) Preparation of phosphate samples for oxygen isotope analysis. *Anal Chem* 63:2397–2400. [https://doi.org/10.1016/0031-0182\(93\)90085-W](https://doi.org/10.1016/0031-0182(93)90085-W)
- D'Errico F, Sánchez Goñi MF (2003) Neandertal extinction and the millennial scale climatic variability of OIS 3. *Quat Sci Rev* 22:769–788. [https://doi.org/10.1016/S0277-3791\(03\)00009-X](https://doi.org/10.1016/S0277-3791(03)00009-X)
- Dansgaard W (1964) Stable isotopes in precipitation. *Tellus XVI*:436–468
- Daura J, Sanz M, Allué E et al (2017) Palaeoenvironments of the last Neanderthals in SW Europe (MIS 3): Cova del Coll Verdaguera (Barcelona, NE of Iberian Peninsula). *Quat Sci Rev* 177:34–56. <https://doi.org/10.1016/j.quascirev.2017.10.005>
- Fagoaga A, Laplana C, Marquina-blasco R et al (2019) Palaeoecological context for the extinction of the Neanderthals : a small mammal study of stratigraphic unit V of the El Salt site, Alcoi, eastern Spain. *Palaeogeogr Palaeoclimatol Palaeoecol* 530:163–175. <https://doi.org/10.1016/j.palaeo.2019.05.007>
- Fagoaga A, Ruiz-Sánchez FJ, Laplana C et al (2018) Palaeoecological implications of Neanderthal occupation at Unit Xb of El Salt (Alcoi, eastern Spain) during MIS 3 using small mammals proxy. *Quat Int* 481:101–112. <https://doi.org/10.1016/j.quaint.2017.10.024>
- Fernández-García M, López-García JM, Bennàsar M et al (2018) Palaeoenvironmental context of Neanderthal occupations in northeastern Iberia: the small-mammal assemblage from Abric Romaní (Capellades, Barcelona, Spain). *Palaeogeogr Palaeoclimatol Palaeoecol* 506:154–167. <https://doi.org/10.1016/j.palaeo.2018.06.031>
- Fernández-García M, López-García JM, Lorenzo C (2016) Palaeoecological implications of rodents as proxies for the Late Pleistocene-Holocene environmental and climatic changes in northeastern Iberia. *CR Palevol* 15:707–719. <https://doi.org/10.1016/j.crpv.2015.08.005>
- Fernández-García M, López-García JM, Royer A et al (2020) Combined palaeoecological methods using small-mammal assemblages to decipher environmental context of a long-term Neanderthal settlement in northeastern Iberia. *Quat Sci Rev* 228:106072. <https://doi.org/10.1016/j.quascirev.2019.106072>
- Fernández-García M, Royer A, López-García JM et al (2019) Unravelling the oxygen isotope signal ( $\delta^{18}O$ ) of rodent teeth from northeastern Iberia, and implications for past climate reconstructions. *Quat Sci Rev* 218:107–121. <https://doi.org/10.1016/j.quascirev.2019.04.035>

- Fernández-Jalvo Y (1992) Tafonomía de microvertebrados del complejo cárstico de Atapuerca (Burgos). Universidad Complutense de Madrid
- Fernández-Jalvo Y, Andrews P (1992) Small mammal taphonomy of Gran Dolina, Atapuerca (Burgos), Spain. *J Archaeol Sci* 19:407–428. [https://doi.org/10.1016/0305-4403\(92\)90058-B](https://doi.org/10.1016/0305-4403(92)90058-B)
- Fernández-Jalvo Y, Andrews P, Denys C et al (2016) Taphonomy for taxonomists: Implications of predation in small mammal studies. *Quat Sci Rev* 139:138–157. <https://doi.org/10.1016/j.quascirev.2016.03.016>
- Fernández-Jalvo Y, Andrews PJ (2016) Atlas of taphonomic identifications: 1001+images of fossil and recent mammal bone modification. Springer, Dordrecht
- Fernández-Jalvo Y, Tormo L, Andrews P, Marin-Monfort MD (2018) Taphonomy of burnt bones from Wonderwerk Cave (South Africa). *Quat Int* 495:19–29. <https://doi.org/10.1016/j.quaint.2018.05.028>
- Finlayson C, Carrión JS (2007) Rapid ecological turnover and its impact on Neanderthal and other human populations. *Trends Ecol Evol* 22:213–222. <https://doi.org/10.1016/j.tree.2007.02.001>
- Finlayson C, Giles Pacheco F, Rodríguez-Vidal J et al (2006) Late survival of Neanderthals at the southernmost extreme of Europe. *Nature* 443:850–853. <https://doi.org/10.1038/nature05195>
- Fletcher WJ, Sánchez-Goni MF (2008) Orbital- and sub-orbital-scale climate impacts on vegetation of the western Mediterranean basin over the last 48,000 yr. *Quat Res* 70:451–464. <https://doi.org/10.1016/j.yqres.2008.07.002>
- Fletcher WJ, Sánchez-Goni MF, Peyron O, Dormoy I (2010) Abrupt climate changes of the last deglaciation detected in a Western Mediterranean forest record. *Clim past* 6:245–264
- Fletcher WJ, Sánchez-Goni MF, Allen JRM et al (2010) Millennial-scale variability during the last glacial in vegetation records from Europe. *Quat Sci Rev* 29:2839–2864. <https://doi.org/10.1016/j.quascirev.2009.11.015>
- Fourel F, Martineau F, Lécuyer C et al (2011) 18O/16O ratio measurements of inorganic and organic materials by elemental analysis–pyrolysis–isotope ratio mass spectrometry continuous-flow techniques. *Rapid Commun Mass Spectrom* 25:2691–2696. <https://doi.org/10.1002/rcm.5056>
- Gehler A, Tütken T, Pack A (2012) Oxygen and carbon isotope variations in a modern rodent community - implications for palaeoenvironmental reconstructions. *PLoS ONE* 7:16–27. <https://doi.org/10.1371/journal.pone.0049531>
- González-Sampériz P, Leroya G, Carrión JS, S et al (2010) Steppes, savannahs, forests and phytodiversity reservoirs during the Pleistocene in the Iberian Peninsula. *Rev Palaeobot Palynol* 162:427–457. <https://doi.org/10.1016/j.revpalbo.2010.03.009>
- Hemming SR (2004) Heinrich events: massive late Pleistocene detritus layers of the North Atlantic and their global climate imprint. *Rev Geophys* 42:RG1005. doi:<https://doi.org/10.1029/2003RG000128>
- Héran MA, Lécuyer C, Legendre S (2010) Cenozoic long-term terrestrial climatic evolution in Germany tracked by  $\delta^{18}\text{O}$  of rodent tooth phosphate. *Palaeogeogr Palaeoclimatol Palaeoecol* 285:331–342. <https://doi.org/10.1016/j.palaeo.2009.11.030>
- Hernández Fernández M (2001) Bioclimatic discriminant capacity of terrestrial mammal faunas. *Glob Ecol Biogeogr* 10:189–204. <https://doi.org/10.1046/j.1466-822x.2001.00218.x>
- Hernández Fernández M, Álvarez Sierra MÁ, Peláez-Campomanes P (2007) Bioclimatic analysis of rodent palaeofaunas reveals severe climatic changes in Southwestern Europe during the Plio-Pleistocene. *Palaeogeogr Palaeoclimatol Palaeoecol* 251:500–526. <https://doi.org/10.1016/j.palaeo.2007.04.015>
- Hewitt GM (2000) The genetic legacy of the Quaternary ice ages. *Nature* 405:907–913. <https://doi.org/10.1038/35016000>
- Higham T, Douka K, Wood R et al (2014) The timing and spatiotemporal patterning of Neanderthal disappearance. *Nature* 512:306–309. <https://doi.org/10.1038/nature13621>
- Hut G (1987) Consultants' group meeting on stable isotope reference samples for geochemical and hydrological investigations, 16–18 Sep. 1985. International Atomic Energy Agency, Vienna
- IAEA/WMO, 2018. Global network of isotopes in precipitation. The GNIP Database. Accessible at WISER (Water Isotope System for Data Analysis, Visualization and Electronic Retrieval): <https://nucleus.iaea.org/wiser>.
- Jones EL (2021) What is a refugium? Questions for the Middle–Upper Palaeolithic transition in peninsular southern Europe. *J Quat Sci* 1–6. <https://doi.org/10.1002/jqs.3274>
- Klevezal GA (2010) Dynamics of incisor growth and daily increments on the incisor surface in three species of small rodents. *Biol Bull-Lettin* 37:836–845. <https://doi.org/10.1134/S1062359010080078>
- Klevezal GA, Ek MPUC, Sukhovskaja LI (1990) Incisor Growth in Voles *Acta Theriol (warsz)* 35:331–344
- Kowalski K (1995) Taphonomy of bats (Chiroptera). *Geobios* 18:251–256. [https://doi.org/10.1016/S0016-6995\(95\)80172-3](https://doi.org/10.1016/S0016-6995(95)80172-3)
- Lagos P (2019) Predation and its effects on individuals: from individual to species. Elsevier Ltd.
- Lécuyer C, Fourel F, Martineau F et al (2007) High-precision determination of 18O/16O ratios of silver phosphate by EA-pyrolysis-IRMS continuous flow technique. *J Mass Spectrom* 42:36–41
- Lécuyer C, Grandjean P, O'Neil JR et al (1993) Thermal excursions in the ocean at the Cretaceous-Tertiary boundary (northern Morocco):  $\delta^{18}\text{O}$  record of phosphatic fish debris. *Palaeogeogr Palaeoclimatol Palaeoecol* 105:235–243. [https://doi.org/10.1016/0031-0182\(93\)90085-W](https://doi.org/10.1016/0031-0182(93)90085-W)
- Lindars ES, Grimes ST, Matthey DP et al (2001) Phosphate  $\delta^{18}\text{O}$  determination of modern rodent teeth by direct laser fluorination: an appraisal of methodology and potential application to palaeoclimate reconstruction. *Geochim Cosmochim Acta* 65:2535–2548
- Lloveras L, Moreno-García M, Nadal J (2008) Taphonomic study of leporid remains accumulated by the Spanish Imperial Eagle (*Aquila adalberti*). *Geobios* 41:91–100. <https://doi.org/10.1016/j.geobios.2006.11.009>
- Lloveras L, Moreno-García M, Nadal J (2012) Feeding the foxes: an experimental study to assess their taphonomic signature on leporid remains. *Int J Osteoarchaeol* 22:577–590. <https://doi.org/10.1002/oa.1280>
- Lloveras L, Moreno-García M, Nadal J (2008) Taphonomic analysis of leporid remains obtained from modern Iberian lynx (*Lynx pardinus*) scats. *J Archaeol Sci* 35:1–13. <https://doi.org/10.1016/j.jas.2007.02.005>
- Longinelli A (1984) Oxygen isotopes in mammal bone phosphate: a new tool for paleohydrological and paleoclimatological research? *Geochim Cosmochim Acta* 48:385–390. [https://doi.org/10.1016/0016-7037\(84\)90259-X](https://doi.org/10.1016/0016-7037(84)90259-X)
- López-García JM, Blain H-A, Bennàsar M et al (2013) Heinrich event 4 characterized by terrestrial proxies in southwestern Europe. *Clim past* 9:1053–1064. <https://doi.org/10.5194/cp-9-1053-2013>
- López-García JM, Blain H-A, Burjachs F et al (2012) A multidisciplinary approach to reconstructing the chronology and environment of southwestern European Neanderthals: the contribution of Teixoneres cave (Moia, Barcelona, Spain). *Quat Sci Rev* 43:33–44. <https://doi.org/10.1016/j.quascirev.2012.04.008>
- López-García JM, Blain HA, Bennàsar M, Fernández-García M (2014) Environmental and climatic context of neanderthal occupation in southwestern Europe during MIS3 inferred from the small-vertebrate assemblages. *Quat Int* 326–327:319–328. <https://doi.org/10.1016/j.quaint.2013.09.010>
- López-García JM, Blain HA, Sanz M, Daura J (2012b) A coastal reservoir of terrestrial resources for neanderthal populations in north-eastern Iberia: Palaeoenvironmental data inferred from the









- small-vertebrate assemblage of Cova del Gegant, Sitges, Barcelona. *J Quat Sci* 27:105–113. <https://doi.org/10.1002/jqs.1515>
- López-García JM, Cuenca-Bescós G, Finlayson C et al (2011) Palaeoenvironmental and palaeoclimatic proxies of the Gorham's cave small mammal sequence, Gibraltar, southern Iberia. *Quat Int* 243:137–142. <https://doi.org/10.1016/j.quaint.2010.12.032>
- López-García JM, Soler N, Maroto J et al (2015) Palaeoenvironmental and palaeoclimatic reconstruction of the Latest Pleistocene of L'Arbreda Cave (Serinyà, Girona, northeastern Iberia) inferred from the small-mammal (insectivore and rodent) assemblages. *Palaeogeogr Palaeoclimatol Palaeoecol* 435:244–253. <https://doi.org/10.1016/j.palaeo.2015.06.022>
- Luz B, Kolodny Y, Horowitz M (1984) Fractionation of oxygen isotopes between mammalian. *Geochim Cosmochim Acta* 48:1689–1693
- Luzi E, López-García JM, Blasco R et al (2017) Variations in *Microtus arvalis* and *Microtus agrestis* (Arvicolinae, Rodentia) dental morphologies in an archaeological context: the case of Teixoneres Cave (Late Pleistocene, North-Eastern Iberia). *J Mamm Evol* 24:495–503. <https://doi.org/10.1007/s10914-016-9355-8>
- Lyman RL (2017) Palaeoenvironmental reconstruction from faunal remains: ecological basics and analytical assumptions. *J Archaeol Res* 1–57. <https://doi.org/10.1007/s10814-017-9102-6>
- Manzanares A (2012) Aves rapaces de la Península Ibérica, Baleares y Canarias. Ediciones Omega, Barcelona
- Marín-Arroyo AB, Rios-Garaizar J, Straus LG et al (2018) Chronological reassessment of the Middle to Upper Paleolithic transition and Early Upper Paleolithic cultures in Cantabrian Spain. *PLoS ONE* 13:1–20. <https://doi.org/10.1371/journal.pone.0194708>
- Maroto J, Julià R, López-García JM, Blain H-A (2012) Chronological and environmental context of the Middle Pleistocene human tooth from Mollet Cave (Serinyà, NE Iberian Peninsula). *J Hum Evol* 62:655–663. <https://doi.org/10.1016/j.jhevol.2012.01.009>
- Mateo-Lomba P, Rivals F, Blasco R, Rosell J (2019) The use of bones as retouchers at Unit III of Teixoneres Cave (MIS 3; Moia, Barcelona, Spain). *J Archaeol Sci Reports* 27:101980. <https://doi.org/10.1016/j.jasrep.2019.101980>
- Mikkola H (1983) Owls of Europe. Buteo Books, Sussex
- Moreno A, Svensson A, Brooks SJ et al (2014) A compilation of Western European terrestrial records 60–8kaBP: towards an understanding of latitudinal climatic gradients. *Quat Sci Rev* 106:167–185. <https://doi.org/10.1016/j.quascirev.2014.06.030>
- Navarro N, Lécuyer C, Montuire S et al (2004) Oxygen isotope compositions of phosphate from arvicoline teeth and Quaternary climatic changes, Gigny, French Jura. *Quat Res* 62:172–182. <https://doi.org/10.1016/j.yqres.2004.06.001>
- Norrdahl K, Korpima E (2002) Seasonal changes in the numerical responses of predators to cyclic vole populations. *Ecography (cop)* 25:428–438
- Ochando J, Amorós G, Carrión JS, et al (2021) Iberian Neanderthals in forests and savannahs. *J Quat Sci* 1–28. <https://doi.org/10.1002/jqs.3339>
- Ochando J, Carrión JS, Blasco R, et al (2020) Neanderthals in a highly diverse, mediterranean-Eurosiberian forest ecotone: the pleistocene pollen record of Teixoneres Cave, northeastern Spain. *Quat Sci Rev* 241. <https://doi.org/10.1016/j.quascirev.2020.106429>
- Olsson V (1979) Studies on a population of Eagle owls in southeast Sweden. *Viltrevy* 11:1–99
- Palomo LJ, Gisbert J, Blanco C (2007) Atlas y libro rojo de los mamíferos terrestres de España. Organismo Autónomo Parques Nacionales, Madrid
- Peneycad E, Candy I, Schreve DC (2019) Variability in the oxygen isotope compositions of modern rodent tooth carbonate: implications for palaeoclimate reconstructions. *Palaeogeogr Palaeoclimatol Palaeoecol* 514:695–705. <https://doi.org/10.1016/J.PAL-AEO.2018.11.017>
- Picin A, Chacón MG, Gómez de Soler B et al (2020) Neanderthal mobile toolkit in short-term occupations at Teixoneres Cave (Moia, Spain). *J Archaeol Sci Reports* 29:102165. <https://doi.org/10.1016/j.jasrep.2019.102165>
- Rasmussen SO, Bigler M, Blockley SP et al (2014) A stratigraphic framework for abrupt climatic changes during the Last Glacial period based on three synchronized Greenland ice-core records: Refining and extending the INTIMATE event stratigraphy. *Quat Sci Rev* 106:14–28. <https://doi.org/10.1016/j.quascirev.2014.09.007>
- Real C, Martínez-varea CM, Carrión Y, et al (2021) Could the central-eastern Iberian Mediterranean region be defined as a refugium? Fauna and flora in MIS 5–3 and their implications for Palaeolithic human behaviour. *J Quat Sci* 1–17. <https://doi.org/10.1002/jqs.3285>
- Rivas-Martínez S (1987) Memoria del Mapa de Series de Vegetación de España. ICONA, Serie Técnica, Madrid
- Rivas-Martínez S, Asensi A, Díez-Garretas B, et al (2007) Mapa de series, geoserias y geopermaseries de vegetación de España. In: Memoria del Mapa de Series de Vegetación de España. Parte I. Itineraria geobotánica, pp 5–436
- Rosell J, Blasco R, Cebrià A, et al (2008) Mossegades i Levallois: les noves intervencions a la Cova de les Teixoneres (Moia, Bages). *Trib d'Arqueologia* 29–43.
- Rosell J, Blasco R, Rivals F et al (2010) Las ocupaciones en la Cova de les Teixoneres (Moia, Barcelona): relaciones espaciales y grado de competencia entre hienas, osos y neandertales durante el Pleistoceno superior. *Zo Arqueol* 13:392–403
- Rosell J, Blasco R, Rivals F et al (2010) A stop along the way: the role of neanderthal groups at level III of Teixoneres cave (Moia, Barcelona, Spain). *Quaternaire* 21:139–154
- Rosell J, Blasco R, Rivals F et al (2017) A resilient landscape at Teixoneres Cave (MIS 3; Moia, Barcelona, Spain): the Neanderthals as disrupting agent. *Quat Int* 435:195–210. <https://doi.org/10.1016/j.quaint.2015.11.077>
- Rosell J, Blasco R, Rivals F et al (2014) Cova del Toll y Cova de les Teixoneres Moia, Barcelona. In: Sala Ramos R (ed) Pleistocene and Holocene hunter-gatherers in Iberia and the Gibraltar Strait: the current archaeological record. Universidad de Burgos, Burgos, pp 302–307
- Royer A, García Yelo BA, Laffont R, Hernández Fernández M (2020) New bioclimatic models for the quaternary palaeoartic based on insectivore and rodent communities. *Palaeogeogr Palaeoclimatol Palaeoecol* 560:110040. <https://doi.org/10.1016/j.palaeo.2020.110040>
- Royer A, Lécuyer C, Montuire S et al (2013) What does the oxygen isotope composition of rodent teeth record? *Earth Planet Sci Lett* 361:258–271. <https://doi.org/10.1016/j.epsl.2012.09.058>
- Royer A, Lécuyer C, Montuire S et al (2014) Summer air temperature, reconstructions from the last glacial stage based on rodents from the site Taillis-des-Coteaux (Vienne), Western France. *Quat Res* 82:420–429. <https://doi.org/10.1016/j.yqres.2014.06.006>
- Royer A, Lécuyer C, Montuire S et al (2013) Late Pleistocene (MIS 3–4) climate inferred from micromammal communities and  $\delta^{18}O$  of rodents from Les Pradelles, France. *Quat Res* 80:113–124. <https://doi.org/10.1016/j.yqres.2013.03.007>
- Royer A, Montuire S, Gilg O, Laroulandie V (2019) A taphonomic investigation of small vertebrate accumulations produced by the snowy owl (*Bubo scandiacus*) and its implications for fossil studies. *Palaeogeogr Palaeoclimatol Palaeoecol* 514:189–205. <https://doi.org/10.1016/j.palaeo.2018.10.018>
- Rozanski K, Araguas-araguas L, Gonfiantini R (1993) Isotopic patterns in modern global precipitation. In: Swart PK, Lohman KC, McKenzie J, Savin S (eds) Climate Change in Continental Isotopic Records. Washington, pp 1–36
- Rufà A, Blasco R, Rivals F, Rosell J (2014) Leporids as a potential resource for predators (hominins, mammalian carnivores, raptors): an example of mixed contribution from level III of



- Teixoneres Cave (MIS 3, Barcelona, Spain). *CR Palevol* 13:665–680. <https://doi.org/10.1016/j.crpv.2014.06.001>
- Rufà A, Blasco R, Rivals F, Rosell J (2016) Who eats whom? Taphonomic analysis of the avian record from the Middle Paleolithic site of Teixoneres Cave (Moià, Barcelona, Spain). *Quat Int* 421:103–115. <https://doi.org/10.1016/j.quaint.2015.06.055>
- Rufi I, Solés A, Soler J, Soler N (2018) Un diente de cría de mamut (*Mammuthus primigenius* Blumenbach 1799, Proboscidea) procedente del Musteriense de la Cueva de la Arbreda (Serinyà, NE de la Península Ibérica). *Estud Geològics* 74:e079. <https://doi.org/10.3989/egcol.43130.478>
- Salamolard M, Butet A, Leroux A, Bretagnolle V (2000) Responses of an avian predator to variations in prey density at a temperature latitude. *Ecology* 81:2428–2441
- Sánchez-Hernández C, Gourichon L, Blasco R, et al (2020a) High-resolution Neanderthal settlements in mediterranean Iberian Peninsula: a matter of altitude? *Quat Sci Rev* 247. <https://doi.org/10.1016/j.quascirev.2020.106523>
- Sánchez-Hernández C, Gourichon L, Soler J et al (2020b) Dietary traits of ungulates in northeastern Iberian Peninsula: did these Neanderthal preys show adaptive behaviour to local habitats during the Middle Palaeolithic? *Quat Int* 557:47–62. <https://doi.org/10.1016/j.quaint.2020.01.008>
- Sánchez-Hernández C, Rivals F, Blasco R, Rosell J (2014) Short, but repeated Neanderthal visits to Teixoneres Cave (MIS 3, Barcelona, Spain): a combined analysis of tooth microwear patterns and seasonality. *J Archaeol Sci* 49:317–325. <https://doi.org/10.1016/j.jas.2014.06.002>
- Sánchez-Hernández C, Rivals F, Blasco R, Rosell J (2016) Tale of two timescales: combining tooth wear methods with different temporal resolutions to detect seasonality of Palaeolithic hominin occupational patterns. *J Archaeol Sci Reports* 6:790–797. <https://doi.org/10.1016/j.jasrep.2015.09.011>
- Schrag DP, Adkins JF, McIntyre K et al (2002) The oxygen isotopic composition of seawater during the Last Glacial Maximum. *Quat Sci Rev* 21:331–342
- Servei Meteorològic de Catalunya, 2018. *Climatologies Comarcals & Anuari de dades meteorològiques*
- Sommer RS, Nadachowski A (2006) Glacial refugia of mammals in Europe: evidence from fossil records. *Mamm Rev* 36:251–265. <https://doi.org/10.1111/j.1365-2907.2006.00093.x>
- Stewart JR, Lister AM, Barnes I, Dalén L (2010) Refugia revisited: individualistic responses of species in space and time. *Proc R Soc B Biol Sci* 277:661–671. <https://doi.org/10.1098/rspb.2009.1272>
- Talamo S, Blasco R, Rivals F et al (2016) The radiocarbon approach to Neanderthals in a carnivore den site: a well-defined chronology for Teixoneres Cave (Moià, Barcelona, Spain). *Radiocarbon* 58:247–256. <https://doi.org/10.1017/RDC.2015.19>
- Terry RC (2007) Inferring predator identity from skeletal damage of small-mammal prey remains. *Evol Ecol Res* 9:199–219
- Tissoux H, Falgueres C, Bahain JJ et al (2006) Datation par les séries de l'uranium des occupations moustériennes de la grotte des Teixoneres (Moià, province de Barcelone, Espagne). *Quaternaire* 17:27–33
- IUCN, 2018. The IUCN Red List of Threatened Species [WWW Document]. Version 2018-2. URL [www.iucnredlist.org](http://www.iucnredlist.org)
- Wolff EW, Chappellaz J, Blunier T et al (2010) Millennial-scale variability during the last glacial: the ice core record. *Quat Sci Rev* 29:2828–2838. <https://doi.org/10.1016/j.quascirev.2009.10.013>
- Wood RE, Arrizabalaga A, Camps M et al (2014) The chronology of the earliest Upper Palaeolithic in northern Iberia: new insights from L'Arbreda, Labeko Koba and La Viña. *J Hum Evol* 69:91–109. <https://doi.org/10.1016/j.jhevol.2013.12.017>
- Zilhão J (2006) Chronostratigraphy of the middle-to-upper palaeolithic transition in the Iberian Peninsula. *Pyrenae* 37:7–84
- Zilhão J (2000) The Ebro frontier: a model for the late extinction of Iberian Neanderthals. In: Stringer CB, Barton RNE, Finlayson C (eds) *Neanderthals on the edge: 150th anniversary conference of the Forbes' Quarry discovery, Gibraltar*. Oxbow Books, Oxford, pp 111–121
- Zilio L, Hammond H, Karampaglidis T et al (2021) Examining Neanderthal and carnivore occupations of Teixoneres Cave (Moià, Barcelona, Spain) using archaeostratigraphic and intra-site spatial analysis. *Sci Rep* 11:1–20. <https://doi.org/10.1038/s41598-021-83741-9>

**Publisher's note** Springer Nature remains neutral with regard to jurisdictional claims in published maps and institutional affiliations.

## Authors and Affiliations

M. Fernández-García<sup>1</sup>  · J. M. López-García<sup>2,3</sup>  · A. Royer<sup>4</sup>  · C. Lécuyer<sup>5,6</sup>  · F. Rivals<sup>2,3,7</sup>  · A. Rufà<sup>8,9</sup>  · R. Blasco<sup>2,3</sup>  · J. Rosell<sup>3,2</sup> 

J. M. López-García  
jmlopez@iphes.cat

A. Royer  
aurelien.royer@u-bourgogne.fr

C. Lécuyer  
christophe.lecuyer@univ-lyon1.fr

F. Rivals  
frivals@iphes.cat

A. Rufà  
arufabonache@gmail.com

R. Blasco  
rblascolopez@gmail.com

J. Rosell  
jordi.rosellardevol@gmail.com

<sup>1</sup> Grupo de I+D+i EVOADAPTA (Evolución Humana y Adaptaciones Económicas y Ecológicas durante la Prehistoria), Dpto. Ciencias Históricas, Universidad de Cantabria, Av. Los Castros 44, 39005 Santander, Spain

<sup>2</sup> Institut Català de Paleocologia Humana i Evolució Social (IPHES-CERCA), Zona Educacional 4, Campus Sescelades URV (Edifici W3), 43007, Tarragona, Spain

<sup>3</sup> Departament d'Història i Història de l'Art, Universitat Rovira i Virgili, Av. Catalunya 35, 43002 Tarragona, Spain

<sup>4</sup> Biogéosciences, UMR CNRS 6282, Université Bourgogne Franche-Comté, 6 Boulevard Gabriel, 21000 Dijon, France

<sup>5</sup> Laboratoire de Géologie de Lyon, UMR CNRS 5276, Université Claude Bernard Lyon 1 and Ecole Normale Supérieure de Lyon, 69622 Villeurbanne, France

<sup>6</sup> Institut Universitaire de France, Paris, France

- <sup>7</sup> ICREA, Pg. Lluís Companys 23, 08010 Barcelona, Spain
- <sup>8</sup> Interdisciplinary Center for Archaeology and Evolution of Human Behaviour (ICArEHB), Campus de Gambelas, FCHS, Universidade do Algarve, 8005-139 Faro, Portugal

- <sup>9</sup> Univ. Bordeaux, CNRS, MCC, PACEA, UMR 5199, F-33600, Pessac, France